Synthesis, Structure, and Reactivity of Zirconium and Hafnium Imido Metalloporphyrins

Joseph L. Thorman,[†] Ilia A. Guzei,[†] Victor G. Young, Jr.,[‡] and L. Keith Woo*[,†]

Departments of Chemistry, Iowa State University, Ames, Iowa 50011-3111, and University of Minnesota, Minneapolis, Minnesota 55455

Received December 7, 1998

The zirconium and hafnium porphyrin imido complexes (TTP)M=NAr$^{i\mathrm{Pr}}$ [TTP = *meso*-tetra-*p*-tolylporphyrinato dianion, M = Zr (**1**), Hf (**2**), Ar$^{i\mathrm{Pr}}$ = 2,6-diisopropylphenyl] were synthesized from (TTP)MCl_2 and 2 equiv of LiNHAr$^{i\mathrm{Pr}}$. The zirconium imido complex, (TTP)Zr=NAr$^{i\mathrm{Pr}}$, was also obtained from the preformed imido complex Zr(NAr$^{i\mathrm{Pr}}$)Cl_2(THF)$_2$ and (TTP)Li_2(THF)$_2$. Treatment of (TTP)$HfCl_2$ with excess LiNH(*p*-MeC_6H_4) resulted in the formation of a bis(amido) complex, (TTP)Hf(NH-*p*-MeC_6H_4)$_2$ (**3**), instead of an imido complex. In the presence of excess aniline, **2** formed an equilibrium mixture of bis(amido) compounds, (TTP)Hf(NHPh)(NHAr$^{i\mathrm{Pr}}$) and (TTP)Hf(NHPh)$_2$. The nucleophilic character of the imido moiety is exhibited by its reaction with ^{t}BuNCO, producing isolable N,O-bound ureato metallacycles. The kinetic product obtained with zirconium, (TTP)Zr(η^2-NAr$^{i\mathrm{Pr}}$C(=N^{t}Bu)O) (**4a**), isomerized to (TTP)Zr(η^2-N^{t}BuC(=NAr$^{i\mathrm{Pr}}$)O) (**4b)** in solution. Upon being heated to 80 °C, **4a** produced the carbodiimide Ar$^{i\mathrm{Pr}}$N=C=N^{t}Bu and a transient Zr(IV) oxo complex. The analogous hafnium complex (TTP)Hf(η^2-NAr$^{i\mathrm{Pr}}$C(=N^{t}Bu)O) (**5a**) did not eject the carbodiimide upon heating to 110 °C but isomerized to (TTP)Hf(η^2-N^{t}BuC(=NAr$^{i\mathrm{Pr}}$)O) (**5b**). To support the formulation of **4a** and **5a** as N,O bound, the complex (TTP)Hf(η^2-NAr$^{i\mathrm{Pr}}$C(=NAr$^{i\mathrm{Pr}}$)O) (**6**) was studied by variable-temperature NMR spectroscopy. The corresponding thio- and selenoureato metallacycles were not isolable in the reaction between **1** and **2** with ^{t}BuNCS and ^{t}BuNCSe. Concomitant formation of the metallacycle with decomposition to the carbodiimide, Ar$^{i\mathrm{Pr}}$N=C=N^{t}Bu, reflects the lower C−Ch bond strength in the proposed N,Ch-bound metallacycles. Treatment of **2** with 1,3-diisopropylcarbodiimide resulted in the η^2-guanidino complex (TTP)Hf(η^2-NAr$^{i\mathrm{Pr}}$C(=N^{i}Pr)N^{i}Pr) (**7a**), which isomerized to the less sterically crowded isomer (TTP)Hf(η^2-N^{i}PrC(=NAr$^{i\mathrm{Pr}}$)N^{i}Pr) (**7b**). Complexes **1**, **2**, **4a**, **4b**, and **7a** were characterized by X-ray crystallography. The monomeric terminal imido compounds, **1** and **2**, are isomorphous: M−N_{imido} distances of 1.863(2) Å (Zr) and 1.859(2) Å (Hf); M−N_{imido}−C angles of 172.5(2)° (Zr) and 173.4(2)° (Hf). The structures of the ureato complexes **4a** and **4b** and the guanidino complex **7a** exhibit typical alkoxido and amido bond distances (Zr−N = 2.1096(13) Å (**4a**), 2.137(3) Å (**4b**); Zr−O = 2.0677(12) Å (**4a**), 2.066(3) Å (**4b**); Hf−N = 2.087(2) Å, 2.151(2) Å (**7a**)).

Introduction

The discovery of C−H bond activation by zirconium imido complexes in 1988 prompted investigations of group 4 imido complexes in a variety of supporting ligand environments.[1,2] Cyclopentadienyl, bulky amido, tetraazaannulene, alkoxo, and bis(amidophosphine) groups have been successfully employed as ancillary ligands for isolable terminal Ti, Zr, and Hf imido complexes.[1−10] Titanium imido compounds rapidly became the most studied of the group 4 compounds and have revealed novel chemistry,[11] including C−H bond activation,[12] [2+2] cycloaddition,[9] and use in titanium nitride film deposition processes.[13] The documented reactivity associated with the M=NR moiety involving zirconium has been more varied. The nucleophilic character of the imido nitrogen has been utilized in hydroamination catalysis,[14] dihydrogen activation,[15] and the formation of a wide variety of metallacycles with substrates ranging from azidotrimethylsilane and benzaldehyde *N*-phenylimine[8] to ethylene.[7] Alkynes, isocyanates, and isocyanides have produced isolable [2+2] cycloaddition products as well (Scheme 1).[1,7,9,16] Studies of hydroamination and hydrocarbon activation involving

[†] Iowa State University.
[‡] X-ray Crystallographic Laboratory, University of Minnesota.

(1) Walsh, P. J.; Hollander, F. J.; Bergman, R. G. *J. Am. Chem. Soc.* **1988**, *110*, 8729.
(2) Cummins, C. C.; Baxter, S. M.; Wolczanski, P. T. *J. Am. Chem. Soc.* **1988**, *110*, 8731.
(3) Profilet, R. D.; Zambrano, C. H.; Fanwick, P. E.; Nash, J. J.; Rothwell, I. P. *Inorg. Chem.* **1990**, *29*, 4362.
(4) Bai, Y.; Roesky, H. W.; Noltemeyer, M.; Witt, M. *Chem. Ber.* **1992**, *125*, 825.
(5) Arney, D. J.; Bruck, M. A.; Huber, S. R.; Wigley, D. E. *Inorg. Chem.* **1992**, *31*, 3749.
(6) Zambrano, C. H.; Profilet, R. D.; Hill, J. E.; Fanwick, P. E.; Rothwell, I. P. *Polyhedron* **1993**, *12*, 689.
(7) Walsh, P. J.; Hollander, F. J.; Bergman, R. G. *Organometallics* **1993**, *12*, 3705.
(8) Meyer, K. E.; Walsh, P. J.; Bergman, R. G. *J. Am. Chem. Soc.* **1995**, *117*, 974.
(9) Blake, A. J.; Mountford, P.; Nikonov, G. I.; Swallow, D. *J. Chem. Soc., Chem. Commun.* **1996**, 1835.
(10) Fryzuk, M. D.; Love, J. B.; Rettig, S. J. *Organometallics* **1998**, *17*, 846.
(11) (a) Wigley, D. E. *Prog. Inorg. Chem.* **1994**, *42*, 239. (b) Mountford, P. *J. Chem. Soc., Chem. Commun.* **1997**, 2127.
(12) Bennett, J. L.; Wolczanski, P. T. *J. Am. Chem. Soc.* **1994**, *116*, 2179 and references therein.
(13) Winter, C. H.; Lewkebandara, T. S.; Prosica, J. W.; Rheingold, A. L. *Inorg. Chem.* **1994**, *33*, 1227.
(14) (a) Walsh, P. J.; Baranger, A. M.; Bergman, R. G. *J. Am. Chem. Soc.* **1992**, *114*, 1708. (b) Baranger, A. M.; Walsh, P. J.; Bergman, R. G. *J. Am. Chem. Soc.* **1993**, *115*, 2753.
(15) Cummins, C. C.; Van Duyne, G. D.; Schaller, C. P.; Wolczanski, P. T. *Organometallics* **1991**, *10*, 164.
(16) Meyer, K. E.; Walsh, P. J.; Bergman, R. G. *J. Am. Chem. Soc.* **1994**, *116*, 2669.

10.1021/ic981399j CCC: $18.00
Published on Web 08/03/1999

Scheme 1

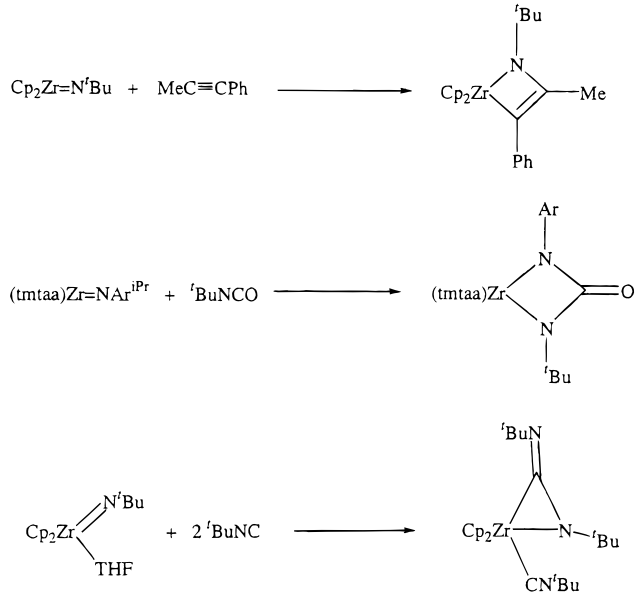

Scheme 2

$$(TTP)TiCl_2 + 2\ LiNHR \rightarrow (TTP)Ti{=}NR + 2\ LiCl + H_2NR$$

$$(TTP)TiCl_2 + \text{excess } H_2N^tBu \rightarrow (TTP)Ti{=}N^tBu + 2\ [H_3N^tBu]Cl$$

$$(TTP)Ti(\eta^2\text{-EtCCEt}) + \tfrac{1}{2}\ PhN{=}NPh \rightarrow (TTP)Ti{=}NPh + EtCCEt$$

$$(TTP)Ti(\eta^2\text{-EtCCEt}) + N_3TMS \rightarrow (TTP)Ti{=}NTMS + N_2$$

$$(TTP)Ti(NPh_2)_2 + H_2N^tBu \rightarrow (TTP)Ti{=}N^tBu + 2\ HNPh_2$$

$$(TTP)TiCl_2 + 2\ LiNPh_2 \rightarrow (TTP)Ti(NPh)_2 + 2\ LiCl$$

$$(TTP)SnCl_2 + 2\ LiNHPh \rightarrow (TTP)Sn(NHPh)_2 + 2\ LiCl$$

$$(TTP)Sn(NHPh)_2 + 2\ H_2Ntolyl \rightarrow (TTP)Sn(NHtolyl)_2 + 2\ H_2NPh$$

zirconium imido complexes illustrate the need for further investigations utilizing different ancillary ligands.[14,17]

We recently explored the chemistry of tetravalent titanium and tin metalloporphyrin complexes containing amido and imido ligands (Scheme 2).[18] The metals in the titanium and tin hexacoordinate complexes reside in the plane of the porphyrin and thus have the ancillary ligands situated in a trans configuration. In comparison, the larger congeners of group 4 have the metal displaced substantially above the porphyrin by ~1 Å. This generates a cis arrangement of unidentate substituents which is slightly more sterically confined relative to that of metallocene analogues.[19] A similar coordination environment is seen in the more flexible and less sterically demanding tetramethyldibenzotetraaza[14]annulene (TMTAA) ligand. For example, the imido complex of Zr(TMTAA) includes a bound pyridine cis to the nitrene group.[20] Monomeric zirconium and hafnium metalloporphyrin chemistry has been explored with a wide variety of ligands, though all are limited to formal single bonds between the metal and ligand.[19] Herein we describe the first isolation and reactivity of zirconium and hafnium metalloporphyrin imido complexes as well as the characterization of N,O-bound ureato(2−) and guanidino(2−) derivatives.

Experimental Section

General Procedures. All manipulations were performed under an inert atmosphere of nitrogen using a Vacuum Atmospheres glovebox equipped with a model MO40-1 Dri-Train gas purifier. All solvents were rigorously degassed and dried prior to use. Benzene-d_6, toluene, and hexane were freshly distilled from purple solutions of sodium benzophenone and brought into the glovebox without exposure to air. The dichloro complexes (TTP)$ZrCl_2$ and (TTP)$HfCl_2$ were prepared according to published procedures[21] but were recrystallized from CH_2Cl_2/hexane prior to use. Commercially purchased compounds, *p*-toluidine, 2,6-diisopropylaniline, ^{t}BuNCO, and ^{t}BuNCS (Aldrich), were dried over activated neutral alumina. The compounds $Zr(Ar^{iPr})Cl_2(THF)_2$,[5] ^{t}BuNCSe,[22] and $LiNHAr^{iPr}$ [5] were prepared from literature procedures. ^{1}H NMR data were recorded at 20.0 °C, unless otherwise stated, on either a Varian VXR (300 MHz) or a Bruker DRX (400 MHz) spectrometer. Chemical shifts were referenced to proton solvent impurities (δ 7.15, C_6D_5H). UV−vis data were recorded on an HP8452A diode array spectrophotometer and are reported as λ_{max} in nm (log ϵ). Elemental analyses (C, H, N) were performed by Iowa State University Instrument Services.

(TTP)Zr=NAr^{iPr}, 1. Method 1. To a toluene solution (ca. 20 mL) of (TTP)$ZrCl_2$ (353 mg, 0.424 mmol) at −25 °C was added a slurry of $LiNHAr^{iPr}$ (166 mg, 0.908 mmol) in toluene (ca. 6 mL). This solution slowly darkened to a red color upon warming to 25 °C. After 2 h, the solution was filtered over Celite. The filtrate was concentrated in vacuo to a black oil. This residue was triturated with hexanes (ca. 12 mL), the mixture was filtered, and the solid was dried in vacuo to afford dark blue **1** (370 mg, 93% yield). Analytically pure crystalline samples could be obtained by layering a toluene solution with hexanes (1:2 v/v), allowing the mixture to stand at −25 °C, filtering, and drying the solid in vacuo. ^{1}H NMR (C_6D_6, 300 MHz): δ 9.17 (s, 8H, β-H), 8.26 (d, 4H, $^3J_{H-H}$ = 8 Hz, *meso*-$C_6H_4CH_3$), 7.97 (d, 4H, $^3J_{H-H}$ = 8 Hz, *meso*-$C_6H_4CH_3$), 7.28 (dd, 8H, $^3J_{H-H}$ = 8 Hz, *meso*-$C_6H_4CH_3$), 6.08 (s, 3H, *m*-, and *p*-C_6H_3), 2.42 (s, 12H, *meso*-$C_6H_4CH_3$), 0.18 (m, 2H, −C*H*Me$_2$), 0.00 (d, 12H, $^3J_{H-H}$ = 7 Hz, −CH*Me*$_2$). ^{13}C NMR (CD_2Cl_2, 400 MHz): δ 153.8, 144.3, 143.6, 142.8, 139.9, 138.9, 137.9, 133.8 (*o*-tolyl), 133.0 (*o*-tolyl), 132.6, 132.4 (β-pyrrole), 130.0, 129.4 (*m*-tolyl), 124.3, 119.5 (*m*-Ar^{iPr}), 115.0 (*p*-Ar^{iPr}), 27.8 (−*C*HMe$_2$), 26.1 (−CH*Me*$_2$), 25.7 (*p*-*Me*C_6H_5). UV−vis (benzene): 544 (4.32), 439 (shoulder, 4.44), 420 (5.56), 398 (shoulder, 4.53). Anal. Calcd for $C_{60}H_{53}N_5Zr$: C, 77.05; H, 5.71; N, 7.49. Found: C, 76.66; H, 5.97; N, 7.02.

Method 2. A round-bottom flask was charged with $Zr(NAr^{iPr})Cl_2(THF)_2$[5] (172 mg, 0.357 mmol) and (TTP)$Li_2(THF)_2$ (119 mg, 0.173 mmol). Toluene (ca. 20 mL) was added, and the reaction mixture was allowed to stir at ambient temperature for 18 h. The dark red solution was filtered over Celite and the filtrate reduced to dryness in vacuo. Recrystallization from toluene/hexanes at −25 °C afforded **1** (126 mg, 78% yield).

(TTP)Hf=NAr^{iPr}, 2. To a rapidly stirred toluene solution (ca. 15 mL) of (TTP)$HfCl_2$ (213 mg, 0.232 mmol) at −25 °C was added a slurry of $LiNHAr^{iPr}$ (90 mg, 0.489 mmol) in toluene (ca. 6 mL). The solution became dark red upon warming to 25 °C over 2 h. The solution was then filtered over Celite. The filtrate was concentrated in vacuo to a black oil. This residue was triturated with hexanes (ca. 12 mL), the mixture was filtered, and the solid was washed with hexanes (4 × 4 mL) and dried in vacuo to afford dark blue **2** (143 mg, 60% yield).

(17) Schaller, C. P.; Cummins, C. C.; Wolczanski, P. T. *J. Am. Chem. Soc.* **1996**, *118*, 591.
(18) (a) Berreau, L. M.; Young, V. G., Jr.; Woo, L. K. *Inorg. Chem.* **1995**, *34*, 527. (b) Gray, S. D.; Thorman, J. L.; Berreau, L. M.; Woo, L. K. *Inorg. Chem.* **1997**, *36*, 278. (c) Gray, S. D., Thorman, J. L.; Adamian, V. A.; Kadish, K. M.; Woo, L. K. *Inorg. Chem.* **1998**, *37*, 1. (d) Chen, J.; Woo, L. K. *Inorg. Chem.* **1998**, *37*, 3269.
(19) Brand, H.; Arnold, J. *Coord. Chem. Rev.* **1995**, *140*, 137.
(20) Blake, A. J.; McInnes, J. M.; Mountford, P.; Nikonov, G. I.; Swallow, D.; Watkin, D. J. *J. Chem. Soc., Dalton Trans.* **1999**, 379.
(21) (a) Kim, H.; Whang, D.; Kim, K.; Do, Y. *Inorg. Chem.* **1993**, *32*, 360. (b) Ryu, S.; Whang, D.; Kim, J.; Yeo, W.; Kim, K. *J. Chem. Soc., Dalton Trans.* **1993**, 205.
(22) Sonoda, N.; Yamamoto, G.; Tsutsum, S. *Bull. Chem. Soc. Jpn.* **1972**, *45*, 2937.

Crystals were grown analogously to **1**. ^{1}H NMR (C_6D_6, 300 MHz): δ 9.17 (s, 8H, β-H), 8.23 (dd, 4H, $^3J_{H-H}$ = 8 Hz, $^2J_{H-H}$ = 2 Hz, *meso*-$C_6H_4CH_3$), 7.97 (dd, 4H, $^3J_{H-H}$ = 8 Hz, $^2J_{H-H}$ = 2 Hz, *meso*-$C_6H_4CH_3$), 7.31 (d, 4H, $^3J_{H-H}$ = 8 Hz, *meso*-$C_6H_4CH_3$), 7.25 (d, 4H, $^3J_{H-H}$ = 8 Hz, *meso*-$C_6H_4CH_3$), 6.16 (d, 2H, $^3J_{H-H}$ = 8 Hz, *m*-C_6H_3), 6.04 (t, 1H, $^3J_{H-H}$ = 8 Hz, *p*-C_6H_3), 2.41 (s, 12H, *meso*-$C_6H_4CH_3$), 0.17 (m, 2H, $-CHMe_2$), 0.00 (d, 12H, $^3J_{H-H}$ = 7 Hz, $-CHMe_2$). UV−vis (benzene): 542 (4.52), 419 (5.67), 397 (shoulder, 4.80). Anal. Calcd for $C_{60}H_{53}N_5Hf$: C, 70.47; H, 5.22; N, 6.85. Found: C, 70.39; H, 5.25; N, 6.54.

(TTP)Hf(NHC$_6$H$_4$-*p*-Me)$_2$, 3. A slurry of (TTP)$HfCl_2$ (253 mg, 0.275 mmol) and LiNH(*p*-MeC_6H_4) (68 mg, 0.60 mmol) in hexanes (ca. 15 mL) was stirred for 10 h at 25 °C, at which time the dark red suspension was filtered. The solid was transferred to a clean fritted filter and washed through with CH_2Cl_2 (2 × 2 mL). The resulting solution was taken to dryness to yield blue microcrystalline **3** (172 mg, 59% yield). ^{1}H NMR (C_6D_6, 300 MHz): δ 9.17 (s, 8H, β-H), 8.24 (d, 4H, $^3J_{H-H}$ = 7 Hz, *meso*-$C_6H_4CH_3$), 7.88 (d, 4H, $^3J_{H-H}$ = 7 Hz, *meso*-$C_6H_4CH_3$), 7.28 (br, 8H, *meso*-$C_6H_4CH_3$), 6.13 (d, 4H, $^3J_{H-H}$ = 8 Hz, *m*-tolyl), 4.27 (d, 4H, $^3J_{H-H}$ = 8 Hz, *o*-tolyl), 2.40 (s, 12H, *meso*-$C_6H_4CH_3$), 1.74 (s, 6H, *p*-MeC_6H_4), 0.96 (s, 2H, N*H*). UV−vis (benzene): 544 (4.44), 418 (5.56), 398 (shoulder, 4.80).

(TTP)Zr(η^2-NAr$^{i\mathrm{Pr}}$C(=N^{t}Bu)O), 4a. A solution of (TTP)Zr=NAr$^{i\mathrm{Pr}}$ (313 mg, 0.334 mmol) and ^{t}BuNCO (250 μL, 2.19 mmol) in toluene (ca. 15 mL) was stirred for 13 h and reduced to dryness in vacuo. The residue was recrystallized from a toluene solution layered with heptane at −25 °C for 1 day to yield microcrystalline dark blue **4a** (112 mg, 32% yield). ^{1}H NMR (C_6D_6, 300 MHz): δ 9.13 (s, 8H, β-H), 8.13 (d, 4H, $^3J_{H-H}$ = 8 Hz, *meso*-$C_6H_4CH_3$), 7.87 (d, 4H, $^3J_{H-H}$ = 8 Hz, *meso*-$C_6H_4CH_3$), 7.29 (dd, 8H, $^3J_{H-H}$ = 8 Hz, *meso*-$C_6H_4CH_3$), 6.79 (t, 1H, $^3J_{H-H}$ = 8 Hz, *p*-C_6H_3), 6.60 (d, 2H, $^3J_{H-H}$ = 8 Hz, *m*-C_6H_3), 2.40 (s, 12H, *meso*-$C_6H_4CH_3$), 0.82 (d, 6H, $^3J_{H-H}$ = 7 Hz, $-CHMe_2$), 0.42 (d, 6H, $^3J_{H-H}$ = 7 Hz, $-CHMe_2$), 0.35 (s, 9H, $NCMe_3$), −0.51 (m, 2H, $-CHMe_2$). ^{13}C NMR (C_6D_6, 400 MHz): δ 152.5, 149.6, 142.7, 140.6, 139.0, 138.0, 135.5, 133.6, 132.8, 127−130 (C_6D_6), 125.6, 123.4, 121.6, 50.4, 30.4, 27.1, 25.2, 24.2, 21.4. UV−vis (toluene): 550 (4.65), 439 (shoulder, 4.94), 418 (5.73). Anal. Calcd for $C_{65}H_{62}N_6OZr$: C, 75.47; H, 6.04; N, 8.12. Found: C, 75.24; H, 6.14; N, 7.94. Exposure to water resulted in rapid decomposition to yield the urea Ar$^{i\mathrm{Pr}}$NHC(O)NH^{t}Bu, as detected by GC/MS: *m*/*z* calcd (found) for $C_{17}H_{28}N_2O$ 276.42 (277). ^{1}H NMR (C_6D_6, 300 MHz): δ 7.16 (m, 1H, *p*-C_6H_3), 7.08 (d, 2H, *m*-C_6H_3), 4.02 (s, 1H, N*H*), 3.57 (m, 2H, $-CHMe_2$), 1.23 (d, 12H, $-CHMe_2$), 1.18 (s, 9H, $N-CMe_3$).

(TTP)Zr(η^2-N^{t}BuC(=NAr$^{i\mathrm{Pr}}$)O), 4b. A solution of (TTP)Zr=NAr$^{i\mathrm{Pr}}$ (330 mg, 0.353 mmol) and Bu^{t}NCO (250 μL, 2.19 mmol) in toluene (ca. 15 mL) was stirred for 13 h and reduced to dryness in vacuo. The residue was recrystallized from toluene/heptane at −25 °C over 17 days. Filtration yielded microcrystalline red **4b**, which was washed with 12 mL of toluene (105 mg, 29% yield). By ^{1}H NMR, 0.5 equiv of toluene was observed as a solvate. ^{1}H NMR (C_6D_6, 400 MHz): δ 9.09 (s, 8H, β-H), 8.23 (d, 4H, $^3J_{H-H}$ = 6 Hz, *meso*-$C_6H_4CH_3$), 7.83 (d, 4H, $^3J_{H-H}$ = 6 Hz, *meso*-$C_6H_4CH_3$), 7.38 (d, 4H, $^3J_{H-H}$ = 6 Hz, *meso*-$C_6H_4CH_3$), 7.25 (d, 4H, $^3J_{H-H}$ = 6 Hz, *meso*-$C_6H_4CH_3$), 6.98 (m, 1H, *p*-C_6H_3), 6.91 (d, 2H, *m*-C_6H_3), 2.41 (s, 12H, *meso*-$C_6H_4CH_3$), 1.84 (spt, 2H, $-CHMe_2$), 0.78 (d, 6H, $^3J_{H-H}$ = 7 Hz, $-CHMe_2$), 0.31 (d, 6H, $^3J_{H-H}$ = 7 Hz, $-CHMe_2$), −0.14 (s, 9H, $NCMe_3$). ^{13}C NMR (C_6D_6, 400 MHz): δ 154.3, 150.1, 145.4, 139.6, 138.0, 137.8, 135.4 (*o*-tolyl), 133.6 (*o*-tolyl), 132.8 (β-pyrrole), 127−129 (solvent), 125.6 (*m*-tolyl), 121.4 (*m*-Ar$^{i\mathrm{Pr}}$), 120.6 (*p*-Ar$^{i\mathrm{Pr}}$), 53.0 ($-CMe_3$), 29.0 (CMe_3), 28.0 ($-CHMe_2$), 23.6 ($-CHMe_2$), 23.1 ($-CHMe_2$), 21.4 (*p*-MeC_6H_5). UV−vis (toluene): 551 (4.31), 4.39 (shoulder, 4.57), 417 (5.46). Anal. Calcd for $C_{68.5}H_{66}N_6OZr$: C, 76.14; H, 6.16; N, 7.78. Found: C, 76.21; H, 6.37; N, 7.32. Exposure to water resulted in rapid decomposition to yield the urea Ar$^{i\mathrm{Pr}}$NHC(O)NH^{t}Bu, as detected by GC/MS.

(TTP)Hf(η^2-NAr$^{i\mathrm{Pr}}$C(=N^{t}Bu)O), 5a. A solution of (TTP)Hf=NAr$^{i\mathrm{Pr}}$ (324 mg, 0.317 mmol) and ^{t}BuNCO (54 μL, 0.473 mmol) in toluene (ca. 10 mL) was stirred for 4.5 h at 25 °C. The solution was filtered, and the filtrate was reduced in vacuo to produce an oily residue. The residue was triturated with 10 mL of hexanes, and the mixture was filtered to yield blue **5a** (228 mg, 64% yield). ^{1}H NMR (C_6D_6, 300 MHz): δ 9.16 (s, 8H, β-H), 8.12 (d, 4H, $^3J_{H-H}$ = 7 Hz, *meso*-$C_6H_4CH_3$), 7.86 (d, 4H, $^3J_{H-H}$ = 7 Hz, *meso*-$C_6H_4CH_3$), 7.29 (dd, 8H, $^3J_{H-H}$ = 7 Hz, *meso*-$C_6H_4CH_3$), 6.77 (t, 1H, *p*-C_6H_3), 6.62 (d, 2H, *m*-C_6H_3), 2.40 (s, 12H, *meso*-$C_6H_4CH_3$), 0.84 (d, 6H, $^3J_{H-H}$ = 7 Hz, $-CHMe_2$), 0.43 (d, 6H, $^3J_{H-H}$ = 7 Hz, $-CHMe_2$), 0.34 (s, 9H, $N-CMe_3$), −0.53 (m, 2H, $-CHMe_2$). ^{13}C NMR (C_6D_6, 400 MHz): δ 151.9, 149.7, 143.5, 140.4, 138.9, 138.0, 135.5 (*o*-tolyl), 133.6 (*o*-tolyl), 133.0 (β-pyrrole), 129−127 (solvent), 125.6, 123.5 (*p*-Ar$^{i\mathrm{Pr}}$), 121.5 (*m*-Ar$^{i\mathrm{Pr}}$), 50.3 ($-CMe_3$), 30.4 ($-CMe_3$), 26.9 ($-CHMe_2$), 25.3 ($-CHMe_2$), 24.4 ($-CHMe_2$), 21.4 (*p*-MeC_6H_5). UV−vis (toluene): 549 (4.40), 416 (5.47). Anal. Calcd for $C_{65}H_{62}N_6OHf$: C, 69.60; H, 5.57; N, 7.49. Found: C, 69.20; H, 5.53; N, 7.30. Exposure to water resulted in rapid decomposition to yield the urea Ar$^{i\mathrm{Pr}}$NHC(O)NH^{t}Bu.

(TTP)Hf(η^2-NAr$^{i\mathrm{Pr}}$C(=NAr$^{i\mathrm{Pr}}$)O), 6. A solution of (TTP)Hf=NAr$^{i\mathrm{Pr}}$ (291 mg, 0.284 mmol) and Ar$^{i\mathrm{Pr}}$NCO (47 μL, 0.412 mmol) in toluene (ca. 40 mL) was stirred for 10 h at 25 °C. The solution was filtered, and the filtrate was reduced in volume (ca. 13 mL) in vacuo. The concentrated solution was layered with hexanes (ca. 13 mL), and the mixture was placed in a freezer at −25 °C overnight. This mixture was filtered and the filtrate reduced to dryness in vacuo. The residue was recrystallized from a toluene solution layered with hexanes at −25 °C overnight. Compound **6** was collected as a dark blue powder (81 mg, 25% yield). ^{1}H NMR (C_7D_8, 400 MHz): δ 9.04 (s, 8H, β-H), 7.84 (d, 4H, $^3J_{H-H}$ = 7 Hz, *meso*-$C_6H_4CH_3$), 7.79 (d, 4H, $^3J_{H-H}$ = 7 Hz, *meso*-$C_6H_4CH_3$), 7.36 (d, 4H, $^3J_{H-H}$ = 7 Hz, *meso*-$C_6H_4CH_3$), 7.29 (d, 4H, $^3J_{H-H}$ = 7 Hz, *meso*-$C_6H_4CH_3$) 6.94 (t, 1H, *p*-C_6H_3), 6.84 (t, 1H, *p*-C_6H_3), 6.79 (d, 2H, *m*-C_6H_3), 6.61 (d, 2H, *m*-C_6H_3), 2.44 (s, 12H, *meso*-$C_6H_4CH_3$), 1.93 (m, 2H, $-CHMe_2$), 0.62 (d, 6H, $-CHMe_2$), 0.44 (d, 6H, $-CHMe_2$), 0.33 (br s, 12H, $-CHMe_2$), −0.07 (m, 2H, $-CHMe_2$). ^{13}C NMR (C_6D_6, 400 MHz): δ 151.5, 149.6, 148.8, 144.1, 140.7, 138.7, 138.6, 138.1, 135.5, 132.9 (β-pyrrole), 132.7, 130−126 (solvent), 125.9, 123.9, 122.0, 121.7, 120.8, 26.9 ($-CHMe_2$), 26.8 ($-CHMe_2$), 26.5 ($-CHMe_2$), 24.7 ($-CHMe_2$), 23.8 ($-CHMe_2$), 21.4 (*p*-MeC_6H_4). UV−vis (toluene): 549 (4.27), 415 (5.45). Anal. Calcd for $C_{73}H_{70}N_6OHf$: C, 71.52; H, 5.76; N, 6.86. Found: C, 69.20; H, 5.53; N, 7.30. This compound appeared pure by ^{1}H NMR, but elemental analyses were routinely low in carbon by 1% or more. Exposure to water resulted in rapid decomposition to yield the urea Ar$^{i\mathrm{Pr}}$NHC(O)NHAr$^{i\mathrm{Pr}}$.

(TTP)Hf(η^2-NAr$^{i\mathrm{Pr}}$C(=N^{i}Pr)N^{i}Pr), 7a. To a stirred solution of **2** (295 mg, 0.288 mmol) in toluene (ca. 12 mL) was added 1,3-diisopropylcarbodiimide (69 μL, 0.441 mmol). The mixture was allowed to stir at ambient temperature for 2 h. This dark red solution was filtered, and the filtrate was reduced to dryness in vacuo. The residue was washed with hexanes (2 × 6 mL) to afford dark blue **7a** (147 mg, 44% yield). Crystals suitable for X-ray diffraction were obtained by recrystallization from a toluene solution layered with hexanes at −25 °C. ^{1}H NMR (C_6D_6, 400 MHz): δ 9.13 (s, 8H, β-H), 8.22 (d, 4H, $^3J_{H-H}$ = 8 Hz, *meso*-$C_6H_4CH_3$), 7.76 (d, 4H, $^3J_{H-H}$ = 8 Hz, *meso*-$C_6H_4CH_3$), 7.35 (d, 4H, $^3J_{H-H}$ = 8 Hz, *meso*-$C_6H_4CH_3$), 7.24 (d, 4H, $^3J_{H-H}$ = 8 Hz, *meso*-$C_6H_4CH_3$), 6.85 (t, 1H, $^3J_{H-H}$ = 8 Hz, *p*-C_6H_3), 6.68 (d, 2H, $^3J_{H-H}$ = 8 Hz, *m*-C_6H_3), 2.40 (s, 12H, *meso*-$C_6H_4CH_3$), 1.63 (m, 1H, $^3J_{H-H}$ = 6 Hz, $NCHMe_2$), 0.96 (d, 6H, $^3J_{H-H}$ = 7 Hz, $C_6H_3CHMe_2$), 0.46 (dd, 12H, $NCHMe_2$ and $C_6H_3CHMe_2$), 0.13 (br d, 7H, $^3J_{H-H}$ = 6 Hz, $NCHMe_2$ and $NCHMe_2$), −0.31 (m, 2H, $^3J_{H-H}$ = 7 Hz, $C_6H_3CHMe_2$). COSY was used to identify protons in overlapping signals. The 2,6-diisopropyl resonances of the NAr$^{i\mathrm{Pr}}$ fragment were definitively assigned by HMBC. ^{13}C NMR (C_6D_6, 200 MHz): δ 152.0, 150.3, 146.1, 142.3 (*o*-Ar$^{i\mathrm{Pr}}$), 139.1, 137.9, 135.3 (*o*-tolyl), 133.7 (*o*-tolyl), 132.8 (β-pyrrole), 130−126 (solvent), 125.3, 122.8 (*p*-Ar$^{i\mathrm{Pr}}$), 122.7 (*m*-Ar$^{i\mathrm{Pr}}$), 47.38, 26.8, 25.6, 24.5, 22.8, 21.4. UV−vis (toluene): 549 (4.32), 416 (5.42). ^{1}H NMR showed that 1 equiv of toluene remained after extended drying in vacuo. Anal. Calcd for $C_{67}H_{67}N_7Hf \cdot C_7H_8$: C, 71.62; H. 6.09; N, 7.90. Found: C, 71.58; H, 6.23; N, 7.70. Exposure to water resulted in rapid decomposition to yield the guanine Ar$^{i\mathrm{Pr}}$NHC(=N^{i}Pr)NH^{i}Pr, as detected by GC/MS: calcd (found) for $C_{19}H_{33}N_3$ *m*/*z* 303.49 (305 [M + H$^+$]).

Reaction of 2 with Aniline. An NMR tube equipped with a Teflon stopcock was charged with **2** (10.36 mg, 10.13 μmol), Ph_3CH (88.5 μL, 0.1397 M, 12.36 μmol) as an internal standard, H_2NPh (2.9 μL, 31.8 μmol), and C_6D_6 (ca. 0.6 mL). This solution was allowed to equilibrate over 11 h at 25 °C, at which time there were present in

solution H_2NAr^{iPr} (9.89 μmol), H_2NPh (14.8 μmol), (TTP)Hf($NHAr^{iPr}$)(NHPh) (1.5 μmol), and (TTP)Hf$(NHPh)_2$ (7.32 μmol). $K = 3.3 \pm 0.3$. ^{1}H NMR (C_6D_6, 400 MHz): δ 9.16 (s, β-H, (TTP)Hf$(NHPh)_2$ and (TTP)Hf(NHPh)($NHAr^{iPr}$)), 8.22 (br d, *meso*-$C_6H_4CH_3$, (TTP)Hf$(NHPh)_2$ and (TTP)Hf(NHPh)$(NAr^{iPr})_2$), 7.86 (br d, *meso*-$C_6H_4CH_3$, (TTP)Hf$(NHPh)_2$ and (TTP)Hf(NHPh)(NAr^{iPr})), 7.26 (br, *meso*-$C_6H_4CH_3$, (TTP)Hf$(NHPh)_2$ and (TTP)Hf(NHPh)(NAr^{iPr})), 6.91 (t, *p*-H_2NArPh), 6.71 (t, *p*-H_2NPh), 6.52 (t, *p*-C_6H_3, (TTP)Hf(NHPh)($NHAr^{iPr}$)), 6.32 (m, *m*-H_2NPh and *m*-NH*Ph*, (TTP)Hf$(NHPh)_2$), 6.06 (m, *p*-HN*Ph*, (TTP)Hf$(NHPh)_2$ and (TTP)Hf(NHPh)($NHAr^{iPr}$)), 4.24 (d, *o*-C_6H_5, (TTP)Hf$(NHPh)_2$), 4.06 (d, *o*-C_6H_5, (TTP)Hf(NHPh)($NHAr^{iPr}$)), 3.16 (br s, H_2NAr^{iPr}), 2.73 (br s, H_2NPh), 2.62 (m, H_2NAr^{iPr}), 2.39 (s, *meso*-$C_6H_4CH_3$), 1.13 (d, H_2NAr^{iPr}), 0.93 (s, (TTP)Hf(N*H*Ph)$_2$ and (TTP)Hf(N*H*Ph)($NHAr^{iPr}$)), 0.38 (d, (TTP)Hf(NHPh)($NHAr^{iPr}$), 0.14 (d, (TTP)Hf(NHPh)($NHAr^{iPr}$), -0.05 (m, (TTP)Hf(NHPh)($NHAr^{iPr}$).

Decomposition of 4a. An NMR tube equipped with a Teflon stopcock was charged with **4a** (11.9 mg, 11.5 μmol), Ph_3CH (87.5 μL, 0.1455 M, 12.73 μmol) as an internal standard, and C_6D_6 (ca. 0.6 mL). After 238 h at 80 °C, **4a** had been consumed and **4b** (1.24 μmol), $[(TTP)ZrO]_2$[23] (0.42 μmol), and $Ar^{iPr}N{=}C{=}N^tBu$ (9.5 μmol, 83% yield by NMR) were detected. ^{1}H NMR (C_6D_6, 300 MHz): δ (for $Ar^{iPr}N{=}C{=}N^tBu$) 7.07 (m, 3H, *m*- and *p*-C_6H_3), 3.64 (spt, 2H, $-CHMe_2$), 1.24 (d, 12H, $-CHMe_2$), 1.18 (s, 9H, N-^{t}Bu); δ (for [(TTP)ZrO]$_2$) 8.74 (s, 8H, β-H), 7.95 (d, 4H, *meso*-$C_6H_4CH_3$), 7.56 (d, 4H, *meso*-$C_6H_4CH_3$), 7.42 (d, 4H, *meso*-$C_6H_4CH_3$), 2.45 (s, 12H, *meso*-$C_6H_4CH_3$).

Decomposition of 4b. An NMR tube equipped with a Teflon stopcock was charged with **4b** (7.32 mg, 7.58 μmol), Ph_3CH (90.0 μL, 0.1455 M, 13.1 μmol) as an internal standard, and C_7D_8 (ca. 0.6 mL). After 228.5 h at 110 °C, **4b** had been consumed and $[(TTP)ZrO]_2$[23] and $Ar^{iPr}N{=}C{=}N^tBu$ (6.96 μmol, 92% yield by NMR) were produced. ^{1}H NMR: δ (for $Ar^{iPr}N{=}C{=}N^tBu$) 3.60 (m, 2H, $-CHMe_2$), 1.23 (d, 12H, $-CHMe_2$), 1.20 (s, 9H, ^{t}Bu), all other signals obscured by solvents; δ (for [(TTP)ZrO]$_2$) 8.69 (s, 16H, β-H), 7.81 (d, 8H, *meso*-$C_6H_4CH_3$), 7.61 (d, 8H, *meso*-$C_6H_4CH_3$), 7.43 (d, 8H, *meso*-$C_6H_4CH_3$), 7.18 (d, 8H, *meso*-$C_6H_4CH_3$), 2.51 (s, 24H, *meso*-$C_6H_4CH_3$).

Reaction of 1 with ^{t}BuNCS. An NMR tube equipped with a Teflon stopcock was charged with **1** (17.43 mg, 18.63 μmol), Ph_3CH (92.0 μL, 0.1397 M, 12.85 μmol) as an internal standard, ^{t}BuNCS (2.8 μL, 23.2 μmol), and C_6D_6 (ca. 0.6 mL). After 21 h at 25 °C, **1** had been consumed and (TTP)Zr(η^2-$NAr^{iPr}C(=N^tBu)S$) (4.33 μmol), $[(TTP)ZrS]_2$ (0.92 μmol), and $Ar^{iPr}N{=}C{=}N^tBu$ (12.35 μmol) were produced. After an additional 70 h at 25 °C, a large amount of brown precipitate was present as well as $[(TTP)ZrS]_2$ (0.21 μmol) and $Ar^{iPr}N{=}C{=}N^tBu$ (16.91 μmol, 91% yield by NMR). ^{1}H NMR (C_6D_6, 300 MHz): δ (for $Ar^{iPr}N{=}C{=}N^tBu$) 7.07 (m, N-2,6-^{i}Pr$_2C_6H_3$), 3.64 (m, N-2,6-^{i}Pr$_2C_6H_3$), 1.24 (d, N-2,6-^{i}Pr$_2C_6H_3$), 1.18 (s, N-^{t}Bu); δ (for [(TTP)Zr(η^2-$NAr^{iPr}C(=N^tBu)S$)]) 9.08 (s, 8H, β-H), 8.30 (d, 4H, *meso*-$C_6H_4CH_3$), 7.69 (d, 4H, *meso*-$C_6H_4CH_3$), 7.35 (d, 4H, *meso*-$C_6H_4CH_3$), 7.21 (d, 4H, *meso*-$C_6H_4CH_3$), 6.96 (t, 1H, *p*-C_6H_3), 6.76 (d, 2H, *m*-C_6H_3), 2.39 (s, 12H, *meso*-$C_6H_4CH_3$), 1.02 (d, 6H, $-CHMe_2$), 0.52 (s, 9H, $NCMe_3$), 0.51 (d, 6H, $-CHMe_2$), -0.13 (m, 2H, $-CHMe_2$); δ (for [(TTP)ZrS]$_2$) 8.74 (s, 8H, β-H), 7.95 (d, 4H, *meso*-$C_6H_4CH_3$), 7.56 (d, 4H, *meso*-$C_6H_4CH_3$), 7.42 (d, 4H, *meso*-$C_6H_4CH_3$), 2.45 (s, 12H, *meso*-$C_6H_4CH_3$).

Reaction of 2 with ^{t}BuNCS. An NMR tube equipped with a Teflon stopcock was charged with **2** (13.88 mg, 13.57 μmol), Ph_3CH (67 μL, 0.1397 M, 9.36 μmol) as an internal standard, ^{t}BuNCS (1.8 μL, 14.90 μmol), and C_6D_6 (ca. 0.6 mL). After 191 h at 25 °C, **2** was still present (0.44 μmol), as well as (TTP)Hf(η^2-$NAr^{iPr}C(=N^tBu)S$) (9.47 μmol), $[(TTP)HfS]_2$ (1.56 μmol), and $Ar^{iPr}N{=}C{=}N^tBu$ (2.75 μmol). The temperature was subsequently raised to 80 °C for 21 h to yield a nearly colorless solution containing $[(TTP)HfS]_2$ (1.36 μmol) and $Ar^{iPr}N{=}C{=}N^tBu$ (12.17 μmol, 90% yield by NMR). ^{1}H NMR (C_6D_6, 300 MHz): δ (for [(TTP)Hf(η^2-$NAr^{iPr}C(=N^tBu)S$)]) 9.12 (s, 8H, β-H), 8.29 (d, 4H, *meso*-$C_6H_4CH_3$), 7.69 (d, 4H, *meso*-$C_6H_4CH_3$), 7.35 (d, 4H, *meso*-$C_6H_4CH_3$), 7.21 (d, 4H, *meso*-$C_6H_4CH_3$), 6.94 (t, 1H, *p*-C_6H_3), 6.77 (d, 2H, *m*-C_6H_3), 2.39 (s, 12H, *meso*-$C_6H_4CH_3$), 1.04 (d, 6H, $-CHMe_2$), 0.52 (s, 9H, $NCMe_3$), 0.51 (d, 6H, $-CHMe_2$), -0.15 (m, 2H, $-CHMe_2$); δ (for $[(TTP)HfS]_2$) 8.75 (s, 8H, β-H), 7.97 (d, 4H, *meso*-$C_6H_4CH_3$), 7.55 (d, 4H, *meso*-$C_6H_4CH_3$), 7.42 (d, 4H, *meso*-$C_6H_4CH_3$), 2.45 (s, 12H, *meso*-$C_6H_4CH_3$).

Reaction of 1 with ^{t}BuNCSe. An NMR tube equipped with a Teflon stopcock was charged with **1** (19.32 mg, 20.66 μmol), Ph_3CH (71 μL, 0.1397 M, 9.92 μmol) as an internal standard, ^{t}BuNCSe (7.5 mg, 46.27 μmol), and C_6D_6 (ca. 0.6 mL). After 8 h at 25 °C, **1** had been consumed and a large amount of brown precipitate had formed. $Ar^{iPr}N{=}C{=}N^tBu$ (17.71 μmol) was produced in 86% yield (by NMR). No intermediates were detected during this reaction.

Reaction of 2 with ^{t}BuNCSe. An NMR tube equipped with a Teflon stopcock was charged with **2** (16.64 mg, 16.27 μmol), Ph_3CH (85 μL, 0.1455 M, 12.37 μmol) as an internal standard, ^{t}BuNCSe (10.1 mg, 62.3 μmol), and C_6D_6 (ca. 0.6 mL). After 109 h at 25 °C, $Ar^{iPr}N{=}C{=}N^tBu$ (13.59 μmol, 84% yield) had formed. No intermediates were detected during this reaction.

Isomerization of 4a to 4b. An NMR tube equipped with a Teflon stopcock was charged with **4a** (23.2 mg, 22.45 μmol), Ph_3CH (90 μL, 0.1397 M, 12.57 μmol), as an internal standard, and C_6D_6 (ca. 0.6 mL). After 912 h at ambient temperature, the progress of the reaction had slowed markedly and only a trace of **4a** remained (0.70 μmol, 97% consumption). Quantification of **4b** was precluded by its insolubility. However, X-ray diffraction quality crystals precipitated during the reaction. No additional products or intermediates were observed throughout this reaction; $t_{1/2} \approx 670$ h.

Isomerization of 5a. An NMR tube equipped with a Teflon stopcock was charged with **5a** (16.86 mg, 15.03 μmol), Ph_3CH (92.5 μL, 0.1397 M, 12.92 μmol), and C_6D_6 (ca. 0.6 mL). After 534 h at 80 °C, the progress of the reaction had slowed markedly and only a trace of **5a** remained. The product, (TTP)Hf(η^2-$N^tBuC(=NAr^{iPr})O$) (14.36 μmol), was present in 94% yield. No additional products or intermediates were observed throughout this reaction; $t_{1/2} \approx 250$ h. ^{1}H NMR (C_6D_6, 300 MHz): δ 9.12 (s, 8H, β-H), 8.24 (br, 4H, *meso*-$C_6H_4CH_3$), 7.83 (br, 4H, *meso*-$C_6H_4CH_3$), 7.38 (br, 4H, *meso*-$C_6H_4CH_3$), 7.26 (br, 4H, *meso*-$C_6H_4CH_3$), 6.93 (m, 3H, *m*- and *p*-C_6H_3), 2.41 (s, 12H, *meso*-$C_6H_4CH_3$), 1.83 (m, 2H, $-CHMe_2$), 0.78 (d, 6H, $^3J_{H-H} = 7$ Hz, $-CHMe_2$), 0.32 (d, 6H, $^3J_{H-H} = 7$ Hz, $-CHMe_2$), -0.14 (s, 9H, $N-CMe_3$).

Isomerization of 7a. Complex **7a** was synthesized in situ in an NMR tube equipped with a Teflon stopcock. The tube was charged with **2** (12.38 mg, 12.10 μmol), ^{i}PrN=C=N^{i}Pr (6.5 μL, 41.5 μmol), Ph_3CH (89 μL, 0.1455 M, 12.95 μmol), and C_6D_6 (ca. 0.6 mL). The formation of **7a** was complete in minutes. The sample was then heated at 80 °C for 488 h; $t_{1/2} \approx 108$ h. The product, (TTP)Hf(η^2-$N^iPrC(=NAr^{iPr})$-N^{i}Pr) (**7b**) (11.67 μmol), was produced in 96% yield (by NMR). No additional products or intermediates were observed throughout this reaction. ^{1}H NMR (C_6D_6, 300 MHz): δ 9.12 (s, 8H, β-H), 8.59 (d, 4H, $^3J_{H-H} = 7$ Hz, *meso*-$C_6H_4CH_3$), 7.76 (d, 4H, $^3J_{H-H} = 7$ Hz, *meso*-$C_6H_4CH_3$), 7.36 (d, 4H, $^3J_{H-H} = 7$ Hz, *meso*-$C_6H_4CH_3$), 7.25 (d, 4H, $^3J_{H-H} = 7$ Hz, *meso*-$C_6H_4CH_3$), 6.69 (d, 2H, *m*-C_6H_3), 6.59 (m, 1H, *p*-C_6H_3), 2.40 (s, 14H, *meso*-$C_6H_4CH_3$ and $NCHMe_2$), 1.62 (spt, 2H, $C_6H_3(CHMe_2)_2$), 0.70 (d, 12H, $^3J_{H-H} = 7$ Hz, $C_6H_3(CHMe_2)_2$), -0.18 (br, 12H, $N-CHMe_2$). The methine proton resonance of the N^{i}Pr group was found by COSY to overlap with the *meso*-$C_6H_4CH_3$ signal at 2.40 ppm. The isopropyl groups were definitively assigned by HMBC.

Structure Determinations of (TTP)Zr=NAr^{iPr} (1), (TTP)Hf=NAr^{iPr} (2), (TTP)Zr($NAr^{iPr}C(=N(^tBu)O)$ (4a), (TTP)Zr($N^tBuC(=N(Ar^{iPr})O)$ (4b), and (TTP)Hf($NAr^{iPr}C(=N^iPr)N^iPr$) (7a). Crystal data are found in Table 1. Compounds **1** and **2** were treated similarly by attachment to a glass fiber and mounting on a Siemens SMART system for data collection at 173(2) K. An initial set of cell constants was calculated from reflections harvested from three sets of 20 frames. These initial sets of frames were oriented such that orthogonal wedges of reciprocal space were surveyed. This produced orientation matrices determined from 208 and 218 reflections for compounds **1** and **2**, respectively. Final cell constants were calculated from sets of 7055 and 8028 strong reflections from the actual data collection, respectively, for **1** and **2**. Three major swaths of frames were collected with 0.30° steps in ω. The data were merged into a unique set as indicated by the data collection ranges. The space groups were determined on the basis of systematic absences and intensity statistics, and a successful direct-methods solution was calculated which provided most non-hydrogen

(23) Thorman, J. L.; Guzei, I. A.; Young, V. G., Jr.; Woo, L. K. Manuscript in submission.

Table 1. Crystal Data

compound	**1**	**2**	**4a**	**4b**	**7a**
empirical formula	$C_{70.50}H_{69}N_5Zr$	$C_{70.50}H_{69}N_5Hf$	$C_{72}H_{74}N_6OZr$	$C_{80}H_{77}N_6OZr$	$C_{67}H_{67}N_7Hf\cdot$toluene
formula weight	1077.53	1164.80	1226.76	1229.70	1274.96
crystal system	monoclinic	monoclinic	triclinic	triclinic	monoclinic
space group	$P2_1/n$	$P2_1/n$	$P\bar{1}$	$P\bar{1}$	$P2_1/c$
a, Å	16.6358(2)	16.6081(2)	13.5421(10)	12.9237(8)	14.8756(8)
b, Å	18.7583(1)	18.6360(3)	15.4623(11)	16.3912(10)	16.7514(9)
c, Å	19.4375(2)	19.3910(1)	16.7239(12)	16.6590(10)	26.1874(15)
α, deg	90	90	98.0192(14)	97.1371(11)	90
β, deg	103.970(1)	104.029(1)	100.8337(14)	105.196(1)	91.796(1)
γ, deg	90	90	113.9894(11)	100.532(1)	90
volume, Å^3	5886.24(10)	5822.67(12)	3050.0(4)	3292.6(3)	6522.4(6)
Z	4	4	2	2	4
ρ, g/cm^3	1.216	1.329	1.337	1.240	1.298
λ, Å	0.710 73	0.710 73	0.710 73	0.710 73	0.710 73
T, K	172(2)	173(2)	173(2)	173(2)	173(2)
μ, mm^{-1}	0.233	1.838	0.229	0.218	1.646
F(000)	2268	2396	1300	1294	2636
θ range, deg	1.45−25.00	1.45−25.06	1.69−28.86	1.28−23.35	1.37−28.34
index ranges	$-19 \le h$ 19	$-19 \le h \le 19$	$-17 \le h \le 18$	$-13 \le h \le 14$	$-15 \le h \le 19$
	$0 \le k \le 22$	$0 \le k \le 22$	$-20 \le k \le 20$	$-17 \le k \le 18$	$-21 \le k \le 21$
	$0 \le l \le 23$	$0 \le l \le 23$	$-20 \le l \le 21$	$-18 \le l \le 17$	$-33 \le l \le 34$
no. of reflections collected	29 098	32 323	19 079	15 220	40 118
no. of independent reflections	10 237	10 215	13 540	9395	15 118
R_{int}	0.0313	0.0270	0.0122	0.0396	0.0352
data/restraints/parameters	10 232/0/694	10 215/0/694	13 540/0/658	9395/37/729	15 115/0/676
R1	0.0403	0.0263	0.0340	0.0547	0.0316
wR2	0.0984	0.0573	0.0910	0.1457	0.0814
GooF	0.977	1.055	0.999	0.995	1.027
largest diff peak and hole, e Å^{-3}	0.305, −0.509	0.444, −1.079	0.491, −0.378	1.032, −0.658	1.414, −1.744

atoms from the E map. Several full-matrix least-squares/difference Fourier cycles were performed that located the remainder of non-hydrogen atoms, which were refined with anisotropic displacement parameters. All hydrogen atoms were placed in ideal positions and refined as riding atoms with relative isotropic displacement parameters. Both complexes were found with one toluene and a half heptane in the unit cell. The heptane was disordered over an inversion center such that three carbons lie on one side and four on the other. Therefore, the third and fourth carbon atoms are terminal methyl groups part of the time. All calculations were performed with SGI INDY R4400-SC and Pentium computers using the SHELXTL V5.0 program suite.[24]

Crystals of **4a**, **4b**, and **7a** were treated in a manner analogous to that for **1** and **2**. Systematic absences in the diffraction data were uniquely consistent for space groups denoted in Table 1. The structures were solved using direct methods, completed by subsequent difference Fourier syntheses and refined by full-matrix least-squares procedures. All non-hydrogen atoms were refined with anisotropic displacement coefficients unless otherwise specified. All hydrogen atoms were treated as idealized contributions. The refinement of **7a** revealed the presence of several disordered solvent molecules. The SQUEEZE filter of the program PLATON[25] was applied to identify and account for 1.5 solvent molecules of toluene present in the asymmetric unit of **7a** along with one molecule of the complex. In the case of **4b**, there are 2.5 molecules of benzene also present in the asymmetric unit. The half-molecule is a part of a benzene molecule residing on an inversion center. The solvent molecules were refined isotropically. The SQUEEZE filter was also applied to **4a** to identify and account for 0.5 toluene molecule and 0.5 heptane molecule present in the asymmetric unit.

Results

Synthesis and Characterization of Imido Complexes. Treatment of *cis*-(TTP)$ZrCl_2$ with 2 equiv of bulky lithium amide reagents, LiNHR (R = 2,4,6-$Me_3C_6H_2$, 2,4,6-$^tBu_3C_6H_2$, 2,4,6-$Ph_3C_6H_2$, 2,6-$^iPr_2C_6H_3$), in toluene resulted in the formation of new terminal imido complexes (eq 1). Of these new

$$(TTP)ZrCl_2 + 2LiNHR \rightarrow (TTP)Zr{=}NR + 2LiCl + NH_2R \quad (1)$$

imido compounds, the 2,6-diisopropylphenyl derivative (TTP)-Zr=NAr^{iPr}, complex **1**, was the most amenable to isolation and purification. The analogous Hf complex, (TTP)Hf=NAr^{iPr}, complex **2**, was also synthesized using the same metathesis reaction. Complex **1** alternatively could be prepared by the reaction of $Zr(NAr^{iPr})Cl_2(THF)_2$[5] with $(TTP)Li_2(THF)_2$. All of these new imido complexes are moisture sensitive. In addition, the Zr imido complexes with mesityl, 2,4,6-tri-*tert*-butylphenyl, and 2,4,6-triphenylphenyl substituents decomposed over time, precluding our ability to isolate analytically pure samples. The rate of this decomposition qualitatively followed the steric bulk of the substituent. However, with 2,6-diisopropylphenyl substituents, complexes **1** and **2** could be kept in the solid state at ambient temperature under an N_2 atmosphere for months. In solution at ambient temperature, complex **2** decomposed to uncharacterized diamagnetic species over a matter of weeks, while **1** was stable in C_6D_6 at elevated temperatures (80 °C) for several days.

The ^{1}H NMR spectra of imido complexes **1** and **2** share the same approximate characteristics. Particularly diagnostic is the porphyrin ring current effect on the imido ligand protons. Consequently, the *meta* and *para* aryl protons of the imido groups exhibit upfield shifts of ∼0.90 ppm relative to that of the free amine. The *meta*, and *para* protons of H_2NAr^{iPr} appear at 7.05 ppm (d) and 6.91 ppm (t), respectively. Thus, a well-separated doublet (6.16 ppm, *m*-H) and triplet (6.04 ppm, *p*-H) for complex **2** is observed. In comparison, complex **1** exhibits a three-proton singlet at 6.08 ppm for the *meta* and *para* Ar^{i}Pr protons. The resonances of the aryl isopropyl groups are also shifted upfield relative to the corresponding free amine resonances at 2.63 ppm (spt) and 1.14 ppm (d). For example, in

(24) *SHELXTL-Plus V5.0*; Siemens Industrial Automation, Inc.: Madison, WI, 1998.
(25) All software and sources of the scattering factors are contained in the SHELXTL V5.10 program library. Sheldrick, G., Siemens XRD, Madison, WI, 1998.

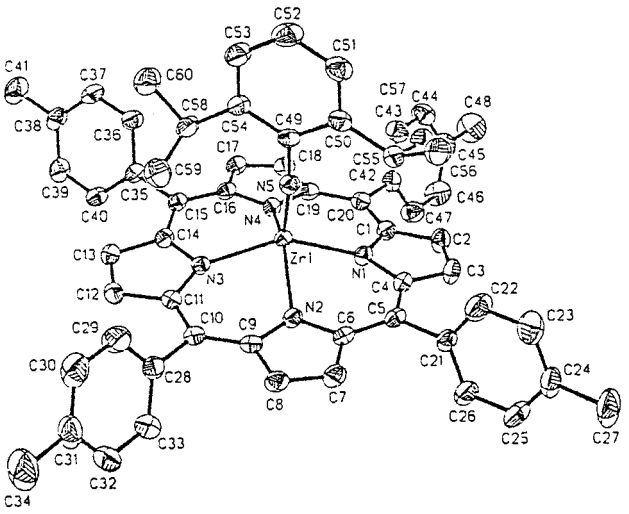

Figure 1. ORTEP representation of (TTP)Zr═NAr$^{i\mathrm{Pr}}$. Thermal ellipsoids are drawn at the 50% probability level.

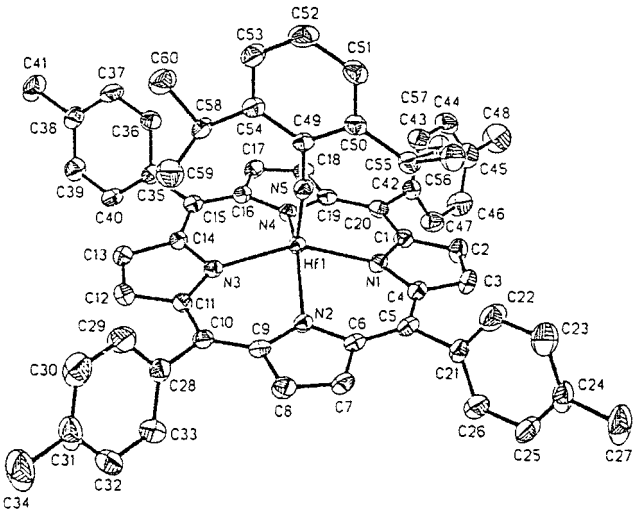

Figure 2. ORTEP representation of (TTP)Hf═NAr$^{i\mathrm{Pr}}$. Thermal ellipsoids are drawn at the 50% probability level.

complex **1**, the methine multiplet appears at 0.18 ppm and the methyl doublet resonates at 0.00 ppm.

The crystal structures of compounds **1** (Figure 1) and **2** (Figure 2) are isomorphous. Each compound cocrystallizes with one toluene and a half heptane per unit cell. As expected, metrical parameters are similar due to the nearly equivalent sizes of the metals. Most structurally characterized five-coordinate Zr and Hf imido complexes have been described as possessing a trigonal-bipyramidal arrangement of the ligands around the metal. The geometry about the metals in complexes **1** and **2** is best described as distorted square-pyramidal. The four pyrrole nitrogens of the porphyrin form the basal plane with average trans pyrrole $N_{por}-M-N_{por}$ angles of 140 and 142°, respectively. Metal$-N_{imido}$ bond lengths are 1.863(2) and 1.859(2) Å for the Zr and Hf complexes, respectively. These values are well within the range of known alkyl- and aryl-substituted imido ligands for Zr and Hf complexes. Typical $M-N_{imido}$ distances are 1.826(4)−1.876(4) Å for zirconium[1,3−6,12] and 1.850(3) Å for hafnium.[6] Only a small deviation from linearity is observed in the M−N5−C49 angles, 172.5(2)° (complex **1**) and 173.4(2)° (complex **2**). Similar metrical features have been reported for the corresponding bond angles of other imido complexes (164.5−179.5° for Zr[1,3−6,12] and 174.4° for Hf[6]). The metal centers in other structurally characterized Zr and Hf metalloporphyrin complexes exhibit coordination numbers from 6 to 8. The range of out-of-plane distances for hexacoordinated Zr(IV) and Hf(IV) porphyrin complexes is 0.84−1.06 Å.[26] In comparison to these examples, the metals in the five-coordinate complexes **1** and **2** reside closer to the plane defined by the four pyrrole nitrogens. The metal atoms in complexes **1** and **2** are located 0.75 and 0.71 Å above the N1−N2−N3−N4 plane, respectively. The smaller value observed for complex **2** is consistent with corresponding values for the congeners [(TPP)Zr(OH)$_2$(O)]$_2$, [(TPP)Hf(OH)$_2$(O)]$_2$ (1.057, 1.048 Å) and (TPP)Zr(O$_2$CCH$_3$)$_2$, (TPP)Hf(O$_2$CCH$_3$)$_2$ (1.036, 1.012 Å).[21,27]

A domed ruffling[28] deformation of the porphyrin macrocycle, a common phenomenon with relatively large metals, is observed in both imido compounds, although to a lesser extent in complex **2**. Deviations from the 24-atom porphyrin plane due to ruffling in complex **1** are 11 (C5), −8 (C10), 19 (C15), and −10 (C20) pm. The resultant dihedral angles in complex **1** of the pyrrole rings containing N1, N2, N3, and N4 relative to the mean 24-atom porphyrin plane are 5.0, −2.6, 5.5, and −8.5°, respectively.

Formation of Bis(amido) Complexes. Treatment of complex **2** with excess aniline results in the complete disappearance of the starting imido complex. Two new bis(amido) complexes, (TTP)Hf(NHPh)$_2$ and (TTP)Hf(NHPh)(NHAr$^{i\mathrm{Pr}}$), are produced as observed by ^{1}H NMR. These two bis(amido) complexes are in equilibrium with the free amines as shown in eq 2 (K = 3.3 ± 0.3). The proton resonances of the coordinated arylamido ligands are shifted upfield. For example, the *o*-H doublet of aniline appears at 6.34 ppm whereas the corresponding *ortho* protons of the amide in (TTP)Hf(NHPh)$_2$ appear at 4.24 ppm. The amide NH protons are found at 0.93 ppm. Thus, in the presence of the less sterically demanding aniline, a bis(amido) complex is produced with concomitant loss of the bulkier (2,6-diisopropylphenyl)amine. Although no new imido complexes were detected by ^{1}H NMR during this reaction, decomposition of the bis(amido) complexes to intractable products was observed over days at ambient temperature. Bulky amines, H$_2$NR (R = 2,4,6-Me$_3$C$_6$H$_2$, 2,4,6-^{t}Bu$_3$C$_6$H$_2$, 2,4,6-Ph$_3$C$_6$H$_2$), do not react with complex **1** or **2**. Treatment of (TTP)HfCl$_2$ with 2 equiv of LiNH(C$_6$H$_4$-*p*-CH$_3$) in hexanes affords the bis(amido) complex (TTP)Hf(NHC$_6$H$_4$-*p*-CH$_3$)$_2$ (**3**). The amide NH protons are readily distinguishable in the ^{1}H NMR spectrum at 0.96 ppm as a sharp singlet integrating as two protons. In free *p*-toluidine the NH protons appear at 2.74 ppm (br s).

$$(\mathrm{TTP})\mathrm{H}(\mathrm{NHAr}^{i\mathrm{Pr}})(\mathrm{NHPh}) + \mathrm{H_2NPh} \rightleftharpoons (\mathrm{TTP})\mathrm{Hf}(\mathrm{NHPh})_2 + \mathrm{H_2NAr}^{i\mathrm{Pr}} \quad (2)$$

[2+2] Condensation Products of Complexes 1 and 2 with R−NCO. Treatment of imido complex **1** with ^{t}BuNCO at ambient temperature resulted in the rapid appearance of a new species, **4a**, which was formulated as an addition product as monitored by ^{1}H NMR. The new compound retains the 2,6-diisopropylphenyl fragment. It also exhibits a new nine-proton singlet at 0.35 ppm consistent with a bound *tert*-butyl group. Moreover, the isopropyl methyl substituents give rise to two

(26) (a) (OEP)ZrCl$_2$, (OEP)Zr(O^{t}Bu)$_2$, and (OEP)ZrMe$_2$: Brand, H.; Arnold, J. *Organometallics* **1993**, *12*, 3655. (b) (OEP)Zr(CH$_2$SiMe$_3$)$_2$: Brand, H.; Arnold, J. *J. Am. Chem. Soc.* **1992**, *114*, 2266. (c) (TPP)Hf(benzenedithiolato): Ryu, S.; Whang, D.; Yeo, H.; Kim, K. *Inorg. Chim. Acta* **1994**, *221*, 51.
(27) Shannon, R. D. *Acta Crystallogr.* **1976**, *A32*, 751.
(28) Jentzen, W.; Simpson, M. C.; Hobbs, J. D.; Song, X.; Ema, T.; Nelson, N. Y.; Medforth, C. J.; Smith, K. M.; Veyrat, M.; Mazzanti, M.; Ramasseul, R.; Marchon, J.-C.; Takeuchi, T.; Goddard, W. A., III.; Shelnutt, J. A. *J. Am. Chem. Soc.* **1995**, *117*, 11085.

new doublets at 0.82 (6H) and 0.42 (6H) ppm. Heating a C_6D_6 solution of **4a** in an NMR probe to 323 K resulted in no broadening of the isopropyl signals. This observation suggested that the isopropyl methyl groups are diastereotopic. Further heating of compound **4a** to 353 K in C_6D_6 for 238 h resulted in the production of 1 equiv of the carbodiimide, ^{t}BuN═C═NAr$^{i\mathrm{Pr}}$. The production of the carbodiimide suggests that compound **4a** can be formulated as an η^2-ureato-*N,O* complex (eq 3). The

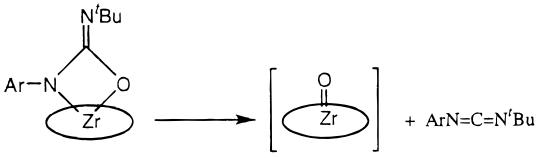

(3)

remaining metal complex was observed transiently by ^{1}H NMR but eventually precipitated out of solution. Initially this complex was formulated as a terminal oxo species, (TTP)Zr═O. However, this putative (TTP)Zr═O complex did not react with excess ^{t}BuNCO to form (TTP)Zr═N^{t}Bu (eq 4).[29] The metal byproduct

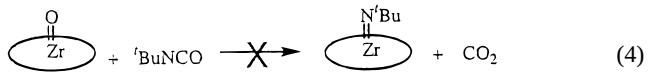

(4)

has been identified as the dimeric species $[(TTP)Zr]_2(\mu\text{-}O)_2$.[23,30]

Over days at 298 K in C_6D_6, complex **4a** isomerizes to a new complex, **4b**. The ureato ligand is still retained as indicated by the presence of *tert*-butyl and isopropyl resonances in the ^{1}H NMR spectrum. However, all proton signals of complex **4b** have shifted relative to those of complex **4a**. For example, the *tert*-butyl resonance of complex **4b** has shifted upfield by 0.49 ppm to −0.14 ppm (s, 9H). The relative change on the isopropyl methyl protons is less drastic. These now appear at 0.31 (d, 6H) and 0.78 ppm (d, 6H). However, a much stronger shift is observed for the methine protons of the isopropyl groups. For complex **4a**, this signal appears at −0.51 ppm. The corresponding resonance for complex **4b** is shifted substantially downfield to 1.84 ppm.

Two candidates serve as possible structures for complex **4b**. These are η^2-N,O- and η^2-N,N-bound ureatos **I** and **II**. The

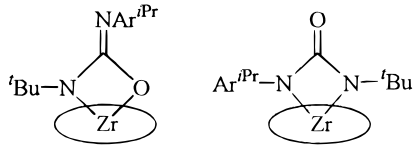

I **II**

strong downfield shift of the isopropyl methine signal suggests that the N-bound aryl group in complex **4b** is further from the porphyrin ring than is its counterpart in complex **4a**. Thus, structure **I** is most likely the correct formulation for complex **4b**. Moreover, heating **4b** at 383 K for 228.5 h resulted in the production of ^{t}BuN═C═NAr$^{i\mathrm{Pr}}$ (92% by NMR). This reactivity is also consistent with the N,O-bound isomer **I**. Final confirmation of the correct structure for complex **4b** was derived from the synthesis of an analogue and by X-ray diffraction analysis (vide infra).

Whereas complex **4a** is formed within minutes at ambient temperature from the reaction of **1** and *tert*-butyl isocyanate, the isomerization of **4a** to **4b** (eq 5) requires ≈38 days at 298

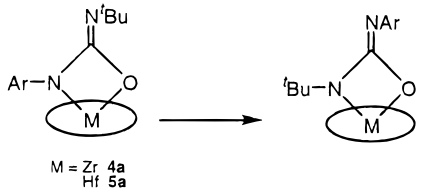

(5)

K in C_6D_6. The production of carbodiimide was not observed during this transformation.

The analogous Hf imido complex **2** also forms a kinetic η^2-ureato-*N,O* complex, **5a**, on treatment with ^{t}BuNCO. The Hf reaction is much slower than that of Zr and takes several hours at 298 K. In addition, **5a** isomerizes to a thermodynamic product, **5b**, after heating at 353 K for 534 h in C_6D_6. Conversion of **5a** to **5b** occurs cleanly with no formation of carbodiimide even at 383 K. The kinetic isomers **4a** and **5a** both share similar spectroscopic characteristics, as do the thermodynamic products **4b** and **5b**. All four complexes, **4a**, **4b**, **5a**, and **5b**, yield the urea ^{t}BuNHC(O)NHAr$^{i\mathrm{Pr}}$ upon hydrolysis.

Treatment of complex **2**, (TTP)Hf═NAr$^{i\mathrm{Pr}}$, with Ar$^{i\mathrm{Pr}}$NCO produced a new adduct, **6**, containing two inequivalent Ar$^{i\mathrm{Pr}}$ fragments. Diagnostic of the two different Ar$^{i\mathrm{Pr}}$ groups are the two unique isopropyl methine signals at 1.93 (m, 2H) and −0.07 ppm (m, 2H). Clearly, complex **6** must be an η^2-N,O-bound ureato. An η^2-N,N-bound ureato ligand would have equivalent Ar$^{i\mathrm{Pr}}$ fragments. Heating complex **6** does not result in conversion to a new isomer. This observation is consistent with all observed isomers of **4** and **5** having N,O-bound ligands.

The two Ar$^{i\mathrm{Pr}}$ groups of complex **6** exhibit different variable-temperature behaviors. The methyl groups of one Ar$^{i\mathrm{Pr}}$ unit give rise to a broad 12-proton signal at 0.33 ppm at 293 K in toluene-d_8. Upon cooling, this broad signal begins to decoalesce at 245 K and eventually sharpens into two new doublets (0.85 and −0.03 ppm) at 234 K, as expected for diastereotopic isopropyl methyl moieties. On warming to 323 K, the methyl signals for this Ar$^{i\mathrm{Pr}}$ fragment sharpen into a single slightly broadened doublet (12H) at 0.31 ppm. The other Ar$^{i\mathrm{Pr}}$ fragment exhibits diastereotopic isopropyl methyl groups with doublets at 0.61 and 0.44 ppm throughout the temperature range from 234 to 323 K. The latter signals are assigned to the Ar$^{i\mathrm{Pr}}$ fragment which is proximal to the porphyrin ligand. The distal Ar$^{i\mathrm{Pr}}$ group is not sterically constrained by the porphyrin macrocycle and can rotate about the N−C_{ipso} bond. The free energy of activation for this rotational process is 12 ± 0.3 kcal/mol.

Synthesis and Isomerization of (TTP)Hf(η^2-NAr$^{i\mathrm{Pr}}$C(═N^{i}Pr)N^{i}Pr). Reaction of complex **2** with a slight excess of 1,3-diisopropylcarbodiimide results in the formation of a new guanidino complex, **7a**. The two *N*-isopropyl groups of **7a** are inequivalent, as indicated by ^{1}H NMR. The proton assignments for this complex were confirmed by HMBC experiments. For example, the methyl proton signal at 0.96 ppm is coupled to an aromatic ^{13}C resonance at 142.3 ppm. Thus, the 0.96 ppm peak

(29) (a) Bryan, J. C.; Burrell, A. K.; Miller, M. M.; Smith, W. H.; Burns, C. J.; Sattelberger, A. P. *Polyhedron* **1993**, *12*, 1769. (b) Legzdins, P.; Phillips, E. C.; Rettig, S. J.; Trotter, J.; Veltheer, J. E.; Yee, V. C. *Organometallics* **1992**, *11*, 3104. (c) Jolly, M.; Mitchell, J. P.; Gibson, V. C. *J. Chem. Soc., Dalton Trans.* **1992**, 1329. (d) Michelman, R. I.; Anderson, R. A.; Bergman, R. G. *J. Am. Chem. Soc.* **1991**, *113*, 5100. (e) Leung, W. H.; Wilkinson, G.; Hussain-Bates, B.; Hursthouse, M. B. *J. Chem. Soc., Dalton Trans.* **1991**, 2791. (f) Herrmann, W. A.; Weichselbaumer, G.; Paciello, R. A.; Fischer, R. A.; Herdtweck, E.; Okuda, J.; Marz, D. W. *Organometallics* **1990**, *9*, 489. (g) Pilato, R. S.; Housemekerides, C. E.; Jernakoff, P.; Rubin, D.; Geoffroy, G. L.; Rheingold, A. L. *Organometallics* **1990**, *8*, 2333. For reviews of RNCO, see: (h) Bruanstein, P.; Nobel, D. *Chem. Rev.* **1989**, *89*, 1927. (i) Cenini, S.; LaMonica, G. *Inorg. Chim. Acta* **1976**, *18*, 279.

(30) Protonolysis of $(OEP)Zr(CH_2SiMe_3)_2$ by 1 equiv of H_2O in $CDCl_3$ generates 2 equiv of $SiMe_4$ and an unisolated complex formulated by ^{1}H NMR as $[(OEP)Zr]_2(\mu\text{-}O)_2$.[26a]

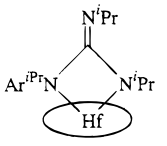

7a

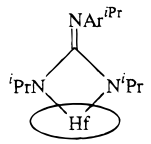

7b

must be associated with an isopropyl fragment of the Ar$^{i\text{Pr}}$ group. The methine protons of these fragments appear at 1.63 (spt, 1H) and 0.13 (spt, 1H) ppm. The upfield methine proton overlaps with one of the methyl signals of the *N*-^{i}Pr group at 0.13 ppm, but was identified by COSY. The *N*-^{i}Pr groups remain inequivalent as the temperature is raised to 323 K. Complex **7a** is clearly an unsymmetrical N,N-bound guanidino species. Over a period of approximately 3 weeks at 353 K in C_6D_6, a new product, **7b**, was formed with the concomitant loss of **7a**. At 323 K, the ^{1}H NMR spectrum (toluene-d_8 solution) of **7b** exhibits a broad peak at −0.17 ppm for the methyl groups of both proximal N^{i}Pr moieties. The distal NAr^{i}Pr displays its isopropyl resonances at 0.70 (d, 12H) and 1.62 (spt, 2H) ppm. Unambiguous assignments for proton resonances were derived from HMBC experiments. The proton peaks at 0.70 (d, 12H) and 1.62 (spt, 2H) ppm are both coupled to an aromatic carbon signal at 137.2 ppm. These two proton resonances correspond to the isopropyl groups of the Ar$^{i\text{Pr}}$ fragment. Consequently, complex **7b** is formulated as the symmetric guanidino complex (TTP)Hf(η^2-N^{i}PrC(=NAr$^{i\text{Pr}}$)N^{i}Pr).

Reaction of Complexes 1 and 2 with ^{t}BuNCS and ^{t}BuNCSe. Imido complexes **1** and **2** undergo reactions with ^{t}BuNCS and ^{t}BuNCSe at a slower rate than the analogous reactions with ^{r}BuNCO. This reflects the greater electrophilic nature of the carbon atom in ^{t}BuNCO relative to ^{t}BuNCS and ^{t}BuNCSe. In the reaction with ^{t}BuNCS, the loss of **1** occurred over 21 h. In the reaction of ^{t}BuNCS with **2**, the presence of the starting imido Hf complex was detected even after 191 h. In both cases, a transient complex assigned as the [2+2] cycloaddition product was observable, but it decomposed simultaneously to the carbodiimide ^{t}BuN=C=NAr$^{i\text{Pr}}$ and sparingly soluble [(TTP)Zr(μ-S)]$_2$. Formulation of the zirconium product as a μ-sulfido-bridged dimer was based on the similarity of its ^{1}H NMR spectrum to that of the oxygen analogue [(TTP)Zr(μ-O)]$_2$. The transient metallacycles were assigned by the similarity of the ^{1}H NMR chemical shifts of the NAr$^{i\text{Pr}}$ and ^{t}Bu groups to those of the oxygen-containing analogues, **4a** and **5a** (Table 2). In the presence of excess ^{t}BuNCSe, **1** and **2** are consumed without the observation of intermediates during the formation of carbodiimide, ^{t}Bu-N=C=NAr$^{i\text{Pr}}$. Once again, the loss of the zirconium imido (8 h) is faster than in the hafnium case (109 h).

Structures of (TTP)Zr(η^2-NAr$^{i\text{Pr}}$C(=N^{t}Bu)O), 4a, (TTP)-Zr(η^2-N^{t}BuC(=NAr$^{i\text{Pr}}$)O), 4b, and (TTP)Hf(η^2-NAr$^{i\text{Pr}}$C(=NPr^i)NPr^i), 7a. The ureato ligand is bound to the zirconium in both **4a** (Figure 3) and **4b** (Figure 4) through nitrogen and oxygen. Both complexes **4a** and **4b** possess a slightly puckered ureato metallacycle. This four-membered ring is nearly perpendicular to the mean 24-atom porphyrin core, with dihedral angles between planes of 91.1° (**4a**) and 101.2° (**4b**). The ureato fragment is staggered with respect to the pyrrole nitrogens. Representative torsional angles are 30.3° (N2−Zr−N6−C49) and 34° (N4−Zr−O−C49) for **4a** and 24.7° (N2−Zr−N5−C49) and 7.7° (N4−Zr−O−C49) for **4b**. The displacements of the Zr atoms from the four-nitrogen pyrrole planes, 0.8891 Å (**4a**) and 0.9069 Å (**4b**), are comparable to those of related six-coordinate compounds (vide supra). For **4a**, the 24-atom porphyrin core exhibits a higher degree of ruffling and doming in comparison to the core of the imido complex **1**. Unexpectedly, very little ruffling is observed in **4b**. Instead, marked doming and an appreciable saddle deformation are seen in the deviations of the β-pyrrole carbon atoms from the 24-atom porphyrin core [2 (C2), 3 (C3), −27 (C7), −26 (C8), 4 (C12), 8 (C13), −20 (C17), −25 (C18) pm]. The metallacycle fragments contain obtuse N−C−O angles of 106.16(14) and 107.1(3)°, as well as acute N−Zr−O angles of 63.62(5) and 63.13(11)°, in **4a** and **4b**, respectively.[29] In comparison to Zr−N amide bond lengths ranging from 2.027(7) to 2.159(3) Å,[31] the Zr−N6 distance in **4a** and the Zr−N5 bond length in **4b** are somewhat elongated with distances of 2.1096(13) and 2.137(3) Å, respectively (Table 2). These bond lengths are slightly shorter than those found for

Table 2. Chemical Shifts of the NAr$^{i\text{Pr}}$ and ^{t}Bu Protons in the N,Ch-Bound Ureato Derivatives

		ppm	
reactant	^{t}BuN=C=E	CH*Me*$_2$, NAr$^{i\text{Pr}}$ from metallacycle complex[a]	^{t}Bu
(TTP)Zr=NAr$^{i\text{Pr}}$ (**1**)	^{t}BuNCO	0.82 (d), 0.42 (d) (**4a**)	0.35 (s)
(TTP)Hf=NAr$^{i\text{Pr}}$ (**2**)	^{t}BuNCO	0.84 (d), 0.43 (d) (**5a**)	0.34 (s)
(TTP)Zr=NAr$^{i\text{Pr}}$ (**1**)	^{t}BuNCS	1.02 (d), 0.51 (d)	0.52 (s)
(TTP)Hf=NAr$^{i\text{Pr}}$ (**2**)	^{t}BuNCS	1.04 (d), 0.51 (d)	0.52 (s)

[a] C_6D_6, 20 °C.

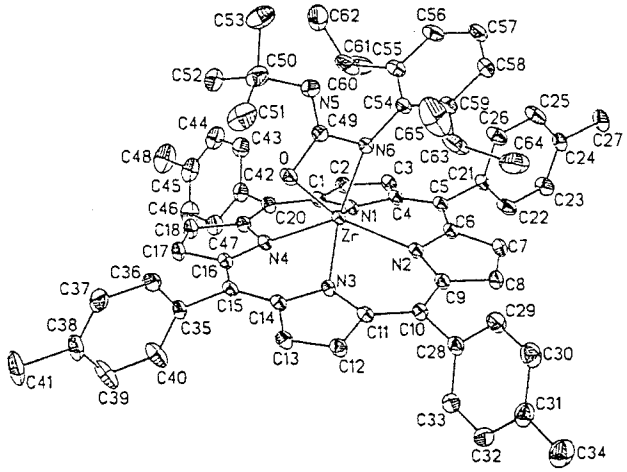

Figure 3. ORTEP representation of (TTP)Zr(η^2-NAr$^{i\text{Pr}}$C(=N^{t}Bu)O). Thermal ellipsoids are drawn at the 30% probability level.

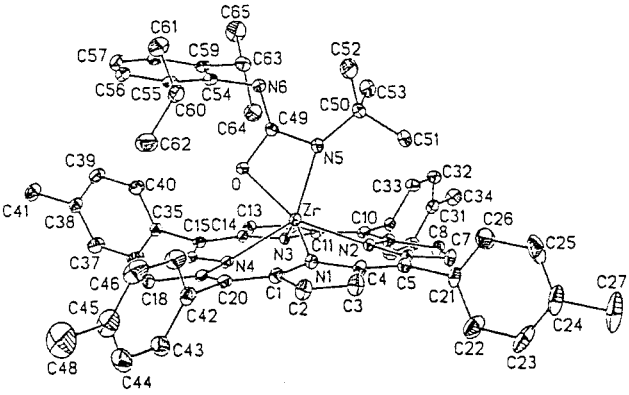

Figure 4. ORTEP representation of (TTP)Zr(η^2-N^{t}BuC(=NAr$^{i\text{Pr}}$)O). Thermal ellipsoids are drawn at the 30% probability level.

(31) (a) Hagen, K.; Holwill, C. J.; Rice, D. A.; Runnacles, J. D. *Inorg. Chem.* **1988**, *27*, 2032. (b) Cardin, D. J.; Lappert, M. F.; Raston, C. L. *Chemistry of Organ-Zirconium and -Hafnium Compounds*; Ellis Horwood Limited: West Sussex, U.K., 1986; p 101.

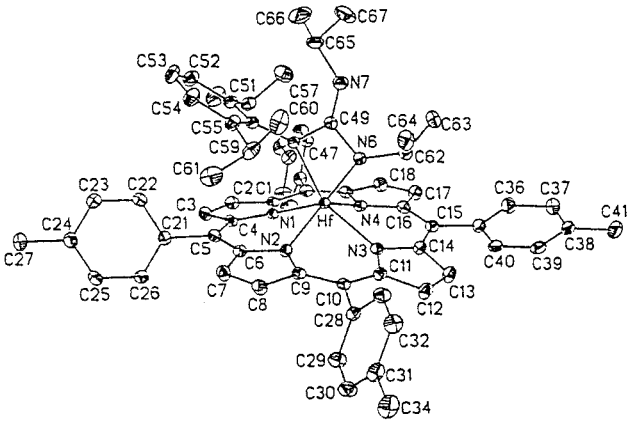

Figure 5. ORTEP representation of (TTP)Hf(η^2-NAr$^{i\mathrm{Pr}}$C(=N^{i}Pr)N$^{i\mathrm{Pr}}$). Thermal ellipsoids are drawn at the 30% probability level.

Table 3. Selected Intramolecular Metallacycle Bond Distances (Å) and Angles (deg) of **4a**, **4b**, and **7a**

complex	Zr−O	M−N$_{amide}$	N$_{amide}$−C49	N$_{imine}$=C49	O−C49
4a	2.0677(12)	2.1096(13)	1.401(2)	1.269(2)	1.349(5)
4b	2.066(3)	2.137(3)	1.387(5)	1.277(5)	1.3530(19)
7a		2.087(2), Hf−N6	1.391(3), N6−C49	1.282(4)	
		2.151(2), Hf−N5	1.428(3), N5−C49		

complex	O−Zr−N	N−Hf−N	E−C49−N$_{amide}$
4a	63.62(5)		106.16(14), E = O
4b	63.13(11)		107.1(3), E = O
7a		63.21(8)	104.0(2), E = N

the N,N′-bound ureato ligand in [Zr(tmtaa)(η^2-NAr^{i}PrC(=O)-N^{t}Bu)]: Zr−N^{i}Pr = 2.168(4) Å and Zr−N^{t}Bu = 2.155(4) Å.[9] No Zr−O π-bonding is suggested by the rather long bond lengths of 2.0677(12) Å in **4a** and 2.066(3) Å in **4b**, along with the acute C49−O−Zr angles of 96.76(10)° in **4a** and 96.7(2)° in **4b**.[31] Other intramolecular metallacycle distances are normal.

The kinetic product from the treatment of complex **2** with 1,3-diisopropylcarbodiimide yields the unsymmetric guanidino-(2−) complex (TTP)Hf(η^2-NAr$^{i\mathrm{Pr}}$C(=N^{i}Pr)N^{i}Pr), **7a**. The slightly puckered Hf(η^2-NAr$^{i\mathrm{Pr}}$C(=N^{i}Pr)N^{i}Pr) metallacyle (Figure 5) is perpendicular to the mean 24-atom porphyrin core, with a dihedral angle between planes of 89.9°. The metallacycle is staggered in relation to the pyrrole nitrogens to a lesser degree than that of the ureato complexes. The torsional angles are 15.9° (N1−Hf−N5−C49) and 5.4° (N3−Hf−N6−C49). The Hf−N^{i}Pr distance (2.087(6) Å) is within known Hf−amido bond distances (2.03−2.12 Å).[32] However, the notably longer Hf−NAr$^{i\mathrm{Pr}}$ distance (2.151(2) Å) may be due to the steric bulk of the Ar$^{i\mathrm{Pr}}$ group. Consequently, there is an irregularity in the Hf−N$_{pyrrole}$ distances: Hf−N1 = 2.251(2) Å, Hf−N2 = 2.184(2) Å, Hf−N3 = 2.238(2) Å, and Hf−N4 = 2.207(2) Å. The two longer distances correspond to the nearly eclipsed nitrogens. Intrametallacycle C−N single- and double-bond distances are typical and are summarized in Table 3. As in complexes **4a** and **4b**, the porphyrin macrocycle of **7a** shows ruffling and doming distortions. However, a somewhat more pronounced saddle deformation is observed, possibly due to the more sterically demanding metallacycle. As expected, the hexacoordinate hafnium center is further out of the N_4 pyrrole plane (0.9111 Å) compared to the five-coordinate hafnium center in the imido complex **2** (out-of-plane distance of 0.7092 Å). The coordination environments most closely resemble a distorted trigonal prism with the metal ion displaced toward one of the rectangular faces.[33]

Discussion

In continuing our work with titanium amido and imido chemistry, we have expanded our efforts to zirconium and hafnium. For hexacoordinate complexes, the large displacements of Zr and Hf from the porphyrin planes confine the two ligands to a *cis* geometry. This places further restrictions on the sizes of the two mutually *cis* ligands. Thus, it is possible to prepare *cis*-(TTP)M(NHC$_6$H$_4$-*p*-CH$_3$)$_2$ (M = Zr, Hf) by simple metathesis reactions of *cis*-(TTP)MCl$_2$ with LiNHAr. However, when ortho substituents are present on the amide reagent, formation of a bis(amido) complex is not observed. Instead, a terminal imido complex is produced. Presumably, *ortho*-substituted arylamides are too bulky to form a *cis*-bis(amido) species. Moreover, the kinetic stability of the final terminal imido complexes is also a function of the size of the *ortho* substituent. Varying the amide aryl group in the reaction of LiNHR (R = 2,4,6-Me$_3$C$_6$H$_2$, 2,4,6-^{t}Bu$_3$C$_6$H$_2$, 2,4,6-Ph$_3$C$_6$H$_2$) with (TTP)-MCl$_2$ led to thermally unstable imido complexes, as observed by ^{1}H NMR. In these cases, analytically pure samples could not be isolated.[34] The 2,4,6-triphenyl derivative, (TTP)Hf=NC$_6$H$_2$Ph$_3$, was isolated as poorly diffracting crystals. A low-resolution molecular structure confirmed the presence of an imido ligand, but the complex was thermally unstable in solution and in the solid state.[35] The steric constraints in the related tetraazaanulene complexes are less demanding. Thus, the formation of a secondary bis(amido) complex, Zr(tmtaa)-(HNAr$^{i\mathrm{Pr}}$)$_2$,[9] is possible.

Examples of isolated N,N′-bound ureato complexes formed from imido complexes have been thoroughly studied.[29] In addition, the similar N,O-bound carbamates are well-known reaction products from [2+2] cycloaddition of isocyantes to oxo species.[29] To the best of our knowledge, there are no examples in the literature of an isolated transition metal N,O-bound ureato-(2−) complex.[36] This is somewhat of an anomaly, since early transition metal M−O bonds are generally stronger than M−N bonds.[37] Nonetheless, the importance of N,O-bound forms has been implicated in the catalytic condensation of phenyl isocyanate to *N,N′*-diphenylcarbodiimide via a proposed vanadium

(32) (a) 2.12 Å average: Hf(=NAr^{i}Pr)(NH(Ar^{i}Pr)$_2$(4-pyrrolidinylpyridine)$_2$ (ref 6). (b) 2.03 Å: Cp*$_2$Hf(H)(NHMe) (Hillhouse, G. L.; Bulls, A. R.; Santarsiero, B. D.; Bercaw, J. E. *Organometallics* **1988**, *7*, 1309). (c) 2.092 Å average: (Me$_4$taen)Hf(NMe$_2$)$_2$ (Black, D. G.; Jordan, R. F.; Rogers, R. D. *Inorg. Chem.* **1997**, *36*, 103). (d) Covalent radii estimates: O = 0.66, N = 0.70 Å (Jolly, W. L. *Modern Inorganic Chemistry*; McGraw-Hill: New York, 1984; p 52). Zr = 1.48, Hf = 1.49, O = 0.73, N = 0.75 Å (Porterfield, W. W. *Inorganic Chemistry*, 2nd ed.; Academic Press: San Diego, CA, 1998; p 214).

(33) For a leading reference pertaining to geometries of d° ML$_6$ complexes, see ref 32c.

(34) For example, during a recrystallization attempt of (TTP)Zr(=NMes*) from toluene/hexanes at −25 °C, approximately 30% decomposed to uncharacterized paramagnetic species.

(35) Thorman, J. L.; Woo, L. K. Unpublished results. *R* value ≈ 13%. At ambient temperature, (TTP)Hf(NPh(Ph)$_3$) crystals decomposed within hours.

(36) (a) Examples of molybdenum and chromium complexes are as follows. N,O-bound ureate(1−): Lam, H. W.; Wilkinson, G.; Hussain-Bates, B.; Hursthouse, M. B. *J. Chem. Soc., Dalton Trans.* **1993**, 781. (b) Synthesis of ((Me$_3$Si)$_2$N)$_2$Sn(NAr^{i}PrC(=NAr^{i}Pr)O) from ((Me$_3$-Si)$_2$N)$_2$Sn(=NAr^{i}Pr) and Ar^{i}PrNCO: Ossig, G.; Meller, A.; Freitag, S.; Herbst-Irmer, R.; Sheldrick, G. M. *Chem. Ber.* **1993**, *126*, 2247.

(37) (a) Ziegler, T.; Tschinke, V.; Versluis, L.; Baerends, E. J.; Ravenek, W. *Polyhedron* **1988**, *7*, 1625. (b) Lappert, M. F.; Patil, D. S.; Pedley, J. B. *J. Chem. Soc., Chem. Commun.* **1975**, 830. (c) Schock, L. E.; Marks, T. J. *J. Am. Chem. Soc.* **1988**, *110*, 7701.

(38) Birdwhistell, K. R.; Boucher, T.; Ensminger, M.; Harris, S.; Johnson, M.; Toporek, S. *Organometallics* **1993**, *12*, 1023.

Scheme 3

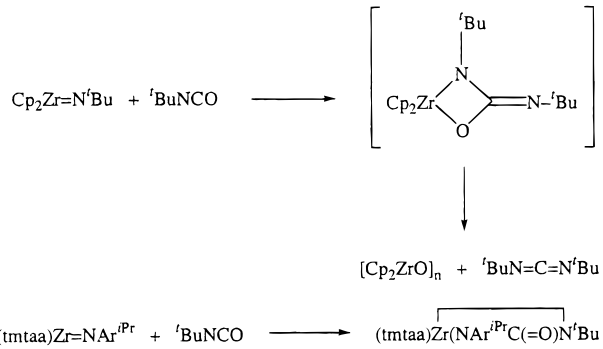

N,O-bound ureato intermediate.[38] Two interesting examples illustrating the reactivity of zirconium imido complexes with ^{t}BuNCO are shown in Scheme 3. The first case involves the implication of an N,O-bound ureate(2−) as an intermediate in the reaction of $Cp_2Zr(N^tBu)$ with ^{t}Bu-NCO. The final products are 1,3-di-*tert*-butylcarbodiimide and $(Cp_2ZrO)_n$.[7] In the second example, treatment of the tetraazaanulene derivative, (tmtaa)-Zr=NAr$^{i\mathrm{Pr}}$, with ^{t}BuNCO yields the N,N-bound ureate.[9] The latter demonstrates the smaller steric demands of the tetraazaannulene ligand in comparison to those of the porphyrin ureato complexes **4a** and **5a**. Mean bond dissociation enthalpy data collected for amido $M(NR_2)_4$ (M = Zr, Hf; R = Me, Et) compounds indicate that Hf−NR_2 bonds are generally stronger than Zr bonds by ≈5%.[39] We propose that the stronger bonds of Hf explain the distinct conditions under which isomerization and decomposition of the ureato complexes **4a** and **5a** occur. Specifically, higher temperatures are required for the isomerization of hafnium complex **5a** (80 °C) versus the zirconium analogue **4a** (25 °C). Similarly, the ejection of carbodiimide occurs for **4a** at 80 °C but does not occur for **5a** at 110 °C.

The anomalous preference of the N,O-binding motif of complexes **4b** and **5b** is presumably a manifestation of steric factors. The N,N′-form is likely to have unfavorable steric interactions between the bulky Ar$^{i\mathrm{Pr}}$ group and the porphyrin. The known N,N′-bound ureato complexes, where steric factors appear not to be as critical, may be dictated by the resultant stronger C=O bond versus the weaker C=N bond required in a N,O-bound ureate.[40] Kinetic products with the bulky Ar$^{i\mathrm{Pr}}$N group proximal to the porphyrin are converted to thermodynamic complexes with the smaller proximal ^{t}BuN group. This steric influence also appears to occur in the isomerization of the guanidino complex **7a**. These isomerizations are readily detected by ^{1}H NMR spectroscopy since the substituents of the metallacycle are strongly affected by the porphyrin ring current as a function of proximity. Under identical reaction conditions, the consumption of imido complexes **1** and **2** by ^{t}BuNCO was found to be complete within minutes for Zr but required ≈90 min for Hf. This difference may be attributed to the slightly more confined coordination sphere due to a smaller out-of-plane distance in **2** relative to the Zr imido analogue. Parallel behavior is seen in the reactions of imido complexes **1** and **2** with ^{t}BuNCS and ^{t}BuNCSe. For the [2+2] metallacycle products from reaction of complexes **1** and **2** with ^{t}BuNC=Ch, the hafnium complexes were found to be more stable toward elimination of carbodiimide. The loss of carbodiimide from **4a** involves the cleavage of M−N and C−O σ-bonds and the formation of a metal−oxygen π-bond and a carbon−nitrogen π-bond. Since the C−O cleavage and C=N formation processes are equivalent for both Zr and Hf, the difference in reactivity lies in the M−N and M=O bonds. Because Hf forms stronger σ-bonds than Zr,[41] **5a** does not eject carbodiimide. The weaker C−S and C−Se bonds in ^{t}BuNCS and ^{t}BuNCSe are manifested in progressively more reactive N,Ch-bound metallacycles with respect to loss of carbodiimide.

In the reactions of **1** and **2** with ^{t}BuNCS and ^{t}BuNCSe, the simultaneous presence of Ar$^{i\mathrm{Pr}}$N=C=N^{t}Bu and the imido complexes does not lead to a guanidino derivative, presumably due to the steric bulk of the carbodiimide. In the presence of the less sterically demanding ^{i}PrN=C=N^{i}Pr, a kinetic [2+2] condensation product, (TTP)Hf(η^2-NAr$^{i\mathrm{Pr}}$C(=N^{i}Pr)N^{i}Pr), **7a**, is formed.[42] As seen with the isocyanate [2+2] analogues, an isomerization slowly occurs which leads to a thermodynamic isomer with the bulky NAr$^{i\mathrm{Pr}}$ moiety at the 3-position of the metallacycle.

The variable-temperature ^{1}H NMR spectra of the guanidino complex **7b** in toluene-d_8 reveal the dynamic aspects involving the imine nitrogen. At 223 K, two doublets for the diastereotopic isopropyl methyl groups are observed for NAr$^{i\mathrm{Pr}}$ at 0.79 and 0.73 ppm. In addition, a doublet is observed for the methyl groups of each N^{i}Pr unit at 0.60 (d, 6H) and −0.82 (d, 6H) ppm. The two resonances arise from a static structure in which one of the N^{i}Pr groups is syn to the aryl fragment. The fact that the syn- and anti-N^{i}Pr groups each exhibit a single doublet indicates that the HfNCN four-membered metallacyclic ring must, on the NMR time scale, have a time-averaged mirror plane of symmetry which bisects the N^{i}Pr groups. Warming the sample to 243 K results in coalescence of the NAr$^{i\mathrm{Pr}}$ isopropyl groups ($\Delta G^{\ddagger} = 11.8 \pm 0.3$ kcal/mol). This resonance subsequently sharpens to a single doublet at temperatures above 253 K. At 283 K, the N^{i}Pr methyl signals have coalesced ($\Delta G^{\ddagger} = 12.1 \pm 0.3$ kcal/mol) and reappear as a sharp doublet (−0.17 ppm) at 363 K. These two coalescence phenomena have equivalent activation barriers and can be explained with a single process involving inversion at the imine nitrogen. The transition state for this process has C_{2v} symmetry which results in NAr$^{i\mathrm{Pr}}$ isopropyl groups that are no longer diastereotopic on the NMR time scale and equivalent N^{i}Pr groups. Rotation about the C_{ipso}−N_{imino} bond can also rationalize the coalescence behavior of the NAr$^{i\mathrm{Pr}}$ isopropyl resonances. Although a rotational process does not need to be invoked, it cannot be definitively ruled out. In the related ureato complex **6**, rotation about the C_{ipso}−N_{imino} bond of the distal NAr$^{i\mathrm{Pr}}$ unit has an activation barrier of 12 kcal/mol.

In a similar manner, the η^2-ureato-*N*,*O* complex **6** also exhibits dynamic ^{1}H NMR features. However, only one of the NAr$^{i\mathrm{Pr}}$ groups exhibits fluxional behavior. Since the NAr$^{i\mathrm{Pr}}$ fragments proximal to the porphyrin in complexes **4a** and **5a** exhibit no fluxionality, the distal NAr$^{i\mathrm{Pr}}$ group in complex **6** must be involved in the dynamic process. Moreover, the only motion that would collapse the diastereotopic ^{i}Pr methyl signals into a single resonance is rotation about the C_{ipso}−N_{imino} bond. The absence of an observable syn−anti isomerization for

(39) $\bar{D}$(Zr−NMe_2) = 83.6 kcal/mol, $\bar{D}$(Hf−NMe_2) = 88.4 kcal/mol: Cardin, D. J.; Lappert, M. F.; Raston, C. L. *Chemistry of Organo-Zirconium and -Hafnium Compounds*; Ellis Horwood Limited: West Sussex, U.K., 1986; pp 16−22.

(40) March, J. *Advanced Organic Chemistry: Reactions, Mechanisms, and Structure*, 4th ed.; Wiley: New York, 1992; p 24.

(41) (a) Ziegler, T.; Tschinke, V.; Versluis, L.; Baerends, E. J.; Ravenek, W. *Polyhedron* **1988**, *7*, 1625. (b) Lappert, M. F.; Patil, D. S.; Pedley, J. B. *J. Chem. Soc., Chem. Commun.* **1975**, 830. (c) Schock, L. E.; Marks, T. J. *J. Am. Chem. Soc.* **1988**, *110*, 7701.

(42) Guanidino(2−): Tin, M. K. T.; Yap, G. P. A.; Richeson, D. S. *Inorg. Chem.* **1998**, *37*, 6728. Guanidino(1−): Gazard, P. A.; Melvyn, K.; Batsanov, A. S.; Howard, J. A. K. *J. Chem. Soc., Dalton Trans.* **1997**, 4625.

complex **6** suggests two possibilities: (1) rapid inversion which is not restricted at the lowest temperature observed (223 K); (2) existence of only one isomer. However, syn−anti inversion barriers of imine units are typically on the order of 10−20 kcal/mol.[43] Also, it is unlikely that the imine inversion barrier in complex **7** is significantly lower than normal. Consequently, the imine fragment in complex **6** must exist in one geometric form. This is not unreasonable, as the two large Ar^{iPr} substituents should prefer to occupy mutually anti sites.

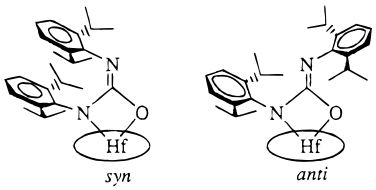

Conclusion

In summary, we have found the rigid basil plane formed by the porphyrin results in novel zirconium and hafnium imido reaction products in comparison to known $L_nM{=}NR$ (M = Zr, Hf) complexes with other supporting ligand systems. Kinetic products from the reaction of RNCO and $^{i}PrN{=}C{=}N^{i}Pr$ with imido complexes **1** and **2** are formed with the NAr^{iPr} moiety remaining bonded to the metal and the heterocumulene-derived nitrene in the distal 3-position of the metallacycle. Distinct isomerization conditions found for **4a** and **5a** illustrate the steric interactions of the porphyrin macrocycle with substituents in the α-position of the metallacycle ligand as well as bonding characteristics between Zr−N and Hf−N. Steric factors appear to be manifested in the conversion of the kinetic isomers to the thermodynamic complexes. Differences in bond strengths between the M−N(amide) bonds (M = Zr, Hf) are exhibited in the requirement of more forcing conditions for isomerization of **5a** relative to **4a**.

The imido complexes also exhibit reactivity with a variety of other heterocumulenes, aldehydes, and ketones. The chemistry of an interesting pinacolone coupling product, (TTP)Zr(η^2-OC(^{t}Bu)(Me)CH=C(^{t}Bu)O), is currently under investigation.[23]

Acknowledgment. We are grateful for support from the Camille and Henry Dreyfus Foundation.

Supporting Information Available: Five X-ray crystallographic files, in CIF format, and tables of crystal data, structure solution and refinement details, atomic coordinates, thermal parameters, and bond distances and angles. This material is available free of charge via the Internet at http://pubs.acs.org.

IC981399J

(43) (a) Patai, S. *The Chemistry of the Carbon-Nitrogen Double Bond*; Interscience Publishers: London, 1970; Chapter 9. (b) Hartwig, J. F.; Bergman, R. G.; Andersen, R. A. *Organometallics* **1991**, *10*, 3344. (c) Knorr, R.; Ruhdorfer, J.; Mehlstaubl, J.; Bohrer, P.; Stephenson, D. S. *Chem. Ber.* **1993**, *126*, 747.